ADVANCED ENERGY MATERIALS
www.advenergymat.de

Prospective Sustainability Screening of Sodium-Ion Battery Cathode Materials

Manuel Baumann, Marcel Häringer, Marius Schmidt, Luca Schneider, Jens F. Peters, Werner Bauer, Joachim R. Binder, and Marcel Weil*

Sodium-ion batteries (SIB) are considered as a promising alternative to overcome existing sustainability challenges related to Lithium-ion batteries (LIB), such as the use of critical and expensive materials with high environmental impacts. In contrast to established LIBs, SIBs are an emerging technology in an early stage of development where a challenge is to identify the most promising and sustainable cathode active materials (CAM) for further research and potential commercialization. Thus, a comprehensive and flexible CAM screening method is developed, providing a fast and comprehensive overview of potential sustainability hotspots for supporting cathode material selection. 42 different SIB cathodes are screened and benchmarked against eight state-of-the-art LIB-cathodes. Potential impacts are quantified for the following categories: i) Cost as ten-year average; ii) Criticality, based on existing raw material criticality indicators, and iii) the life cycle carbon footprint. The results reveal that energy density is one of the most important factors in all three categories, determining the overall material demand. Most SIB CAM shows a very promising performance, obtaining better results than the LIB benchmark. Especially the Prussian Blue derivatives and the manganese-based layered oxides seem to be interesting candidates under the given prospective screening framework.

1. Introduction

A major goal of post-lithium battery research is to reduce the sustainability impacts associated with the increasing demand for electrochemical energy storage systems. These post-lithium systems include a wide set of cell chemistries such as Mg, Al, Na, Ka, or Zn systems, with the name given according to the shuttling ion within the battery.[1,2] Especially, Sodium-Ion batteries (SIB) are considered as a promising alternative in this regard, avoiding the use of critical and expensive materials with high environmental impacts.[3–5] Sharing their 50-year history but also most properties with LIB, SIBs are considered as drop-in technology with a wide set of potential cathode material candidates.[6] One of their advantages over LIBs is the use of sodium instead of lithium for active materials and electrolytes and the possibility to apply aluminum instead of copper as current collector.[7] While the larger ionic radius of sodium and its lower standard electrode potential (−2.71 V vs Standard Hydrogen Electrode (SHE) as compared to −3.02 V vs SHE for lithium)[5,8] leads to lower energy densities, they are able to cover similar application fields,[9] with several companies already commercializing SIB.[10–13]

For both technologies, cathode active materials (CAM) based on intercalation reactions are required that allow to reversibly insert a high amount of the corresponding guest species (Na^+ or Li^+) and thus achieve high energy densities and lifetimes. Consequently, the selection of the CAM determines the later application of a battery,[8] but often also is the main driver of costs and environmental impacts.[14,15] The most prominent CAM for present LIBs are, among others, $LiNi_{0.6}Mn_{0.2}Co_{0.2}O_2$ (Lithium Nickel Manganese Cobalt (NMC) 622) and $LiFePO_4$ (Lithium Iron Phosphate (LFP)). For SIB, at a lower technological maturity level, numerous material combinations are being researched with different properties in

M. Baumann, M. Weil
Institute for Technology Assessment and Systems Analysis
KIT – ITAS
76021 Karlsruhe, Germany
E-mail: manuel.baumann@kit.edu

The ORCID identification number(s) for the author(s) of this article can be found under https://doi.org/10.1002/aenm.202202636.

DOI: 10.1002/aenm.202202636

M. Häringer, M. Schmidt, L. Schneider, W. Bauer, J. R. Binder
Institute for Applied Materials – Energy Storage Systems
KIT – IAM-ESS
76344 Karlsruhe, Germany

J. F. Peters
University of Alcalá (UAH)
Department of Economics
Alcalá de Henares
28801 Madrid, Spain

M. Weil
Helmholtz-Institute for Electrochemical Energy Storage
KIT – HIU
89081 Ulm, Germany

terms of energy density, cycle lifetime, coulombic efficiency or cost, but also resource availability/criticality and environmental impacts. Numerous studies are available on the technical development of different SIB technologies considering a wide set of CAM.[6,8,15,16] However, most of these studies focus on technical or performance aspects (e.g., energy densities, cycles lifetimes, efficiency), but do not provide wider views on potential sustainability implications related to different CAM in early development stages.

This work provides a comprehensive and highly flexible CAM screening including over 40 material compositions, giving a quick but inclusive overview of potential sustainability hotspots for SIB in early-stage research. All screened SIB cathodes are benchmarked against state-of-the-art LIB CAM under consideration of costs, material criticality, and carbon footprint (CF).

2. State of the Art

2.1. Sodium-Ion Cathode Types and Materials

Analog to LIB, SIB CAM can be separated into layered oxides and polyanionic materials. In the following, a brief overview of different CAM types is provided. Detailed insights into the properties of different materials can be found in existing works.[8,16–19]

2.1.1. Layered Oxides

Layered oxide materials are prominently used as CAM for commercial LIB, and their counterparts for SIB have been successfully tested and improved on lab-scale in recent years.[20] The structure can be generally described as Na_xTMO_2 (**TM**, transition metal, e.g., Mn, Fe, Ni, Co, Ti, etc.). In order to distinguish the layered oxides further, they can be indicated with the letters "P" and "O" referring to a prismatic and octahedral coordination of Na between the layers. The sodium diffusion in a prismatic layer follows a direct path, while in an octahedral layer it follows the interstitial sites in a zigzag pattern (indirect diffusion).[20] The number of transition metal layers per unit cell of the crystal lattice is indicated as a numeral after the letters P/O.

As an example, P2 and O3 can be named as two important and well-known types of layered oxides (e.g., Na_xTMO_2 (P2) for prismatic two-layer).[18,21] P2 types show in general a higher initial discharge capacity (vs Na-anode) but a less stable cycling stability than O3. In both cases of P and O type layered oxides, manganese and iron are the most prominent transition metals for good electrochemical performance. With the combination of different amounts of these two and other transition metals, higher capacity and stability can be achieved. Average working potentials rank from 2.4 to 3.6 V and typical practical capacities are in the range of 100–200 mAh g^{-1}.[20]

2.1.2. Polyanionic Materials

The second group of CAM is the polyanionic materials. They can be expressed with the general formula $Na_xTM_y(XO_4)_n$ whereby ***X*** could represent S, P, Si, As, Mo, or W and **TM** is a transition metal.[22] They consist of a series of tetrahedron anionic units $(XO_4)^{n-}$ or their derivatives $(X_mO_{3m+1})^{n-}$ and TMO_x polyhedra with strong covalent bonds.[23] The polyanionic CAM exhibit three key characteristics: First, there is the high redox potential caused by the unique inductive effect.[24,25] Second, they show a high thermal stability, favorable for safety issues. Third, they exhibit a low electric conductivity, typical for NASICON-structured materials.[26,27] While the former two characteristics convert them into promising CAM, research is ongoing to overcome the drawback of the low conductivity by applying various strategies such as carbon coating, reducing particle size, or designing the optimal particle morphology.[28–32] A second group of polyanionic CAM is the Prussian Blue Analogues (PBA) with the general chemical formula $Na_{2-x}TM_a[TM_b(CN)_6]_{1-y}\ zH_2O$. These can be synthesized at low temperatures[33] and rely on typically abundant materials. TM_a and TM_b could be two different or the same transition metal, whereby Fe is the most famous representative. $Na_{0.61}Fe[Fe(CN)_6]_{0.94}$ is a promising candidate which shows an energy density of 493 mAh g^{-1}.[34]

2.2. Early Stage Sustainability Assessment of Na-Ion Batteries and Materials

Being costs, material demand, and sustainability among the principal drivers for the development of SIB, a crucial question in this context is how to steer these efforts before technology entrenchment limits the potential for adopting the technology towards more sustainability.[4] Typically, such an exercise is relevant in early technology development stages, with the efforts for adjustments increasing with advancing technology readiness levels (TRLs).[35] For batteries, these TRLs have been specifically adopted as Battery Component Readiness Level (BC-RL) 1 to 9 alongside checklists for known factors, possible projections, and fully unknown factors for each level.[36] Using more general Battery Technology Readiness Levels (BTRL), three system analysis levels (SAL) can be identified and classified as shown in **Figure 1**: i) simple screening methods based on available and often uncertain data able to compare a high magnitude of alternatives on a component level; ii) prospective assessments on a device level (e.g., cells) using parametric and analogous (in reference to similar technologies) approaches for the conceptual stage with limited data and high uncertainty and iii) full assessments using an engineering-driven approach where detailed engineering and manufacturing estimates and corresponding data (material, equipment, energy demand) are available.[37] The arrows indicate that system analysis can be seen as an iterative process at the corresponding BTRL levels. SIB can be classified within a BTRL between 1 to 6, although some SIB types have already reached higher BTRL of up to 7.[10–13] LIB in contrast can be considered to be mature and fully available in markets, beyond BTRL 9.

A high number of potential SIB material combinations are tested in the electrochemical development stage (BTRL 1-4). Being the experience with LIB is not directly transposable to SIB due to their different electrochemical characteristics, knowledge about the potential impacts of the material candidates is sought for supporting decision making at this stage. This requires the definition of selection criteria and corresponding models that are flexible, modular, and easy to

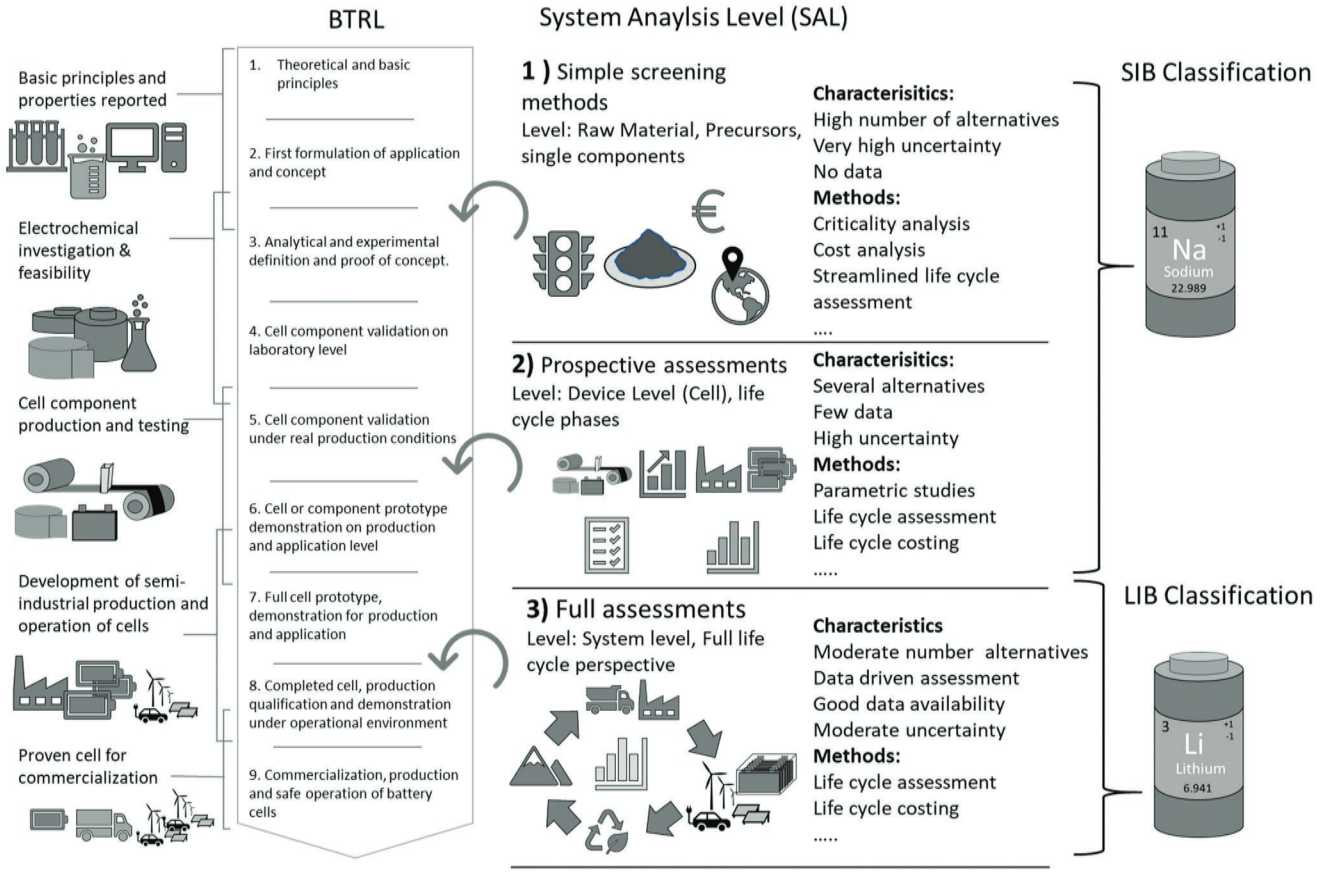

Figure 1. BTRL (TRL inspired by)[35] dependent SAL, including a description of characteristics and applied method on each SAL. LIBs are considered to be situated at BTRL 7+, while SIBs are at an earlier BTRL.

communicate if, for example, new material candidates are tested. Here, screening methods can be applied, such as simple cost estimations, environmental footprinting, toxicity, and raw material criticality analysis providing first insights into potential hotspots of single components like electrodes and electrolytes.[38] A typical indicator on SAL 1 is supply risk (SR) which describes the likelihood of supply disruption considering processing, smelting, and refining capacities which are often similarly concentrated in producing countries.[39] Alternatively, life cycle assessment (LCA) approaches can be used, providing a broader picture by considering a selected set of impact categories as in the case of for nanoscale cathode materials for LIB.[40]

While costs, material and environmental aspects of LIB have been extensively assessed,[41,42] there are only a few publications available that take a close look into general sustainability aspects of specific SIB materials. These include the potential cost competitiveness of SIB compared to current LIB,[43] analyzes of raw material availability,[5] and potential SR,[44] and potential environmental impacts and cost of SIB compared to LIB.[4,7,45–47] Apart from the mentioned studies, a good review in this regard is provided in a recent work,[48] which is why the individual studies are not discussed further here.

Typically, these works start from BC RL >4 using SAL 2 methods such as LCA or Life Cycle Costing (LCC). These are powerful tools to analyze a limited set of electrode materials and compare them with state-of-the-art technologies, pinpointing hotspots and improvement potentials under the considered aspects. However, LCA studies require time intensive data gathering in the phase of building up a life cycle inventory. This might be problematic if insufficient data is available due to the early technology development stages and limits the number of options that can be assessed in a single study. To the best of the authors' knowledge, only a very limited set of the potentially suitable CAM for SIB in relation to sustainability have been assessed so far although information about the potentially most promising CAM can help to guide CAM research and development toward more sustainably batteries.

3. Methodology

In order to tackle the need for early-stage assessment of SIB materials, a comprehensive and flexible CAM screening method has been developed. It provides a fast overview of potential cost and criticality hotspots using SAL 1 within a BTRL of 1–6 and benchmarks them against state-of-the-art LIB technologies. Used indicators are CAM cost, CF, and material criticality in form of an SR, which have been selected based on literature and on dedicated workshops with involved material researchers. An overview of the entire methodology including

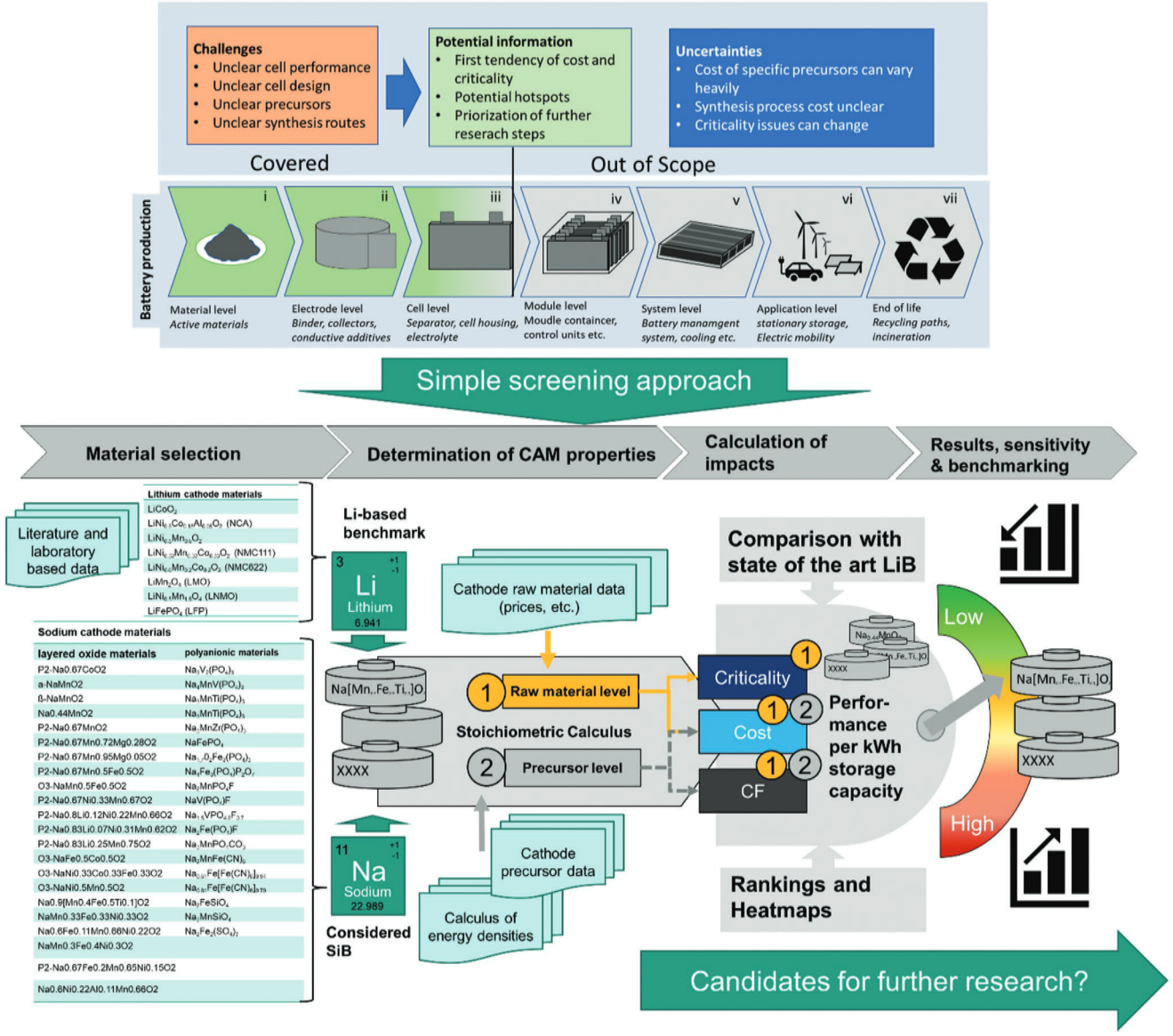

Figure 2. Outline of the applied screening methodology.

all considered CAM types is provided in **Figure 2** and described in the following.

3.1. Material Selection

The CAM to be screened are selected based on an exhaustive literature screening combined with input from workshops with material researchers within the KIT. A total of 49 CAM are identified for consideration in the assessment, and categorized according to Section 2.2 into polyanionic and layered oxide insertion materials. Their specific composition and properties such as mass and required precursors are obtained directly from the literature review, complemented by their own laboratory data and stoichiometric calculations.

3.2. Determination of CAM Properties

The specific energy of a CAM is the product of its specific capacity and average potential. The theoretical specific capacity Q_{th} can be calculated as follows:

$$Q_{th} = F * z/M \quad (1)$$

With F being the faraday constant, z the exchanged electrons per mole, and M the molar mass of the considered CAM. If not all ions are de-/intercalated from/into the considered material within a certain voltage window, the theoretical capacity does not reflect its actual capacity. To take this into account, the specific energy is calculated based on the specific reversible capacities obtained from the literature. If no information was available on the reversible capacity and/or the average potential, it

Table 1. Overview of parameters considered for the calculation of specific capacities for different anode materials.

	Li	Na	Graphite	Hard carbon
Ua,anode [V]	0	0	0.1	0.2
Q,anode [mAh g^{-1}]	3861	1166	360	330

was taken from the integral of the potential-capacity curve. Note that the reversible capacity can also be higher than the theoretical capacity if more ions intercalate in the discharge cycle and then de-intercalate in the first charge cycle (this is only possible in half cells or pre-sodiated full cells with an excess of ions). The specific energies (W) are calculated as follows:

for half-cells:

$$W = Q_{\text{cathode}}\, U_{\text{a,cathode}} \tag{2}$$

for full cells:

$$W = \frac{Q_{\text{cathode}} * \left(U_{\text{a,cathode}} - U_{\text{a,anode}}\right)}{1 + \frac{Q_{\text{cathode}}}{Q_{\text{anode}}}} \tag{3}$$

With $Q_{\text{cathode/anode}}$ being the reversible specific capacity of the cathode/anode, and $U_{\text{a,cathode/anode}}$ is the average potential of the cathode/anode (see **Table 1**). More details about the determination of the average potential and capacity of the anode materials are provided in the Supporting Information.

The obtained reversible specific energy of the different CAM is provided in **Table 2** as follows: i) energy density without anode; ii) versus metallic lithium (LIB) or sodium (SIB); and iii) versus graphite (LIB) or hard carbon (HC) (SIB). Note that the energy densities provided here are considering only the active material and not the entire electrode, current collector, electrolyte, separator, or packaging. Considering inactive materials on an electrode level (binders, conductive additives, current collectors, etc.) would lead to a decrease in specific energies. This effect is relevant not only for cells (housing, separator), but also on module level (container, control units, sensors, etc.) and finally system level (cooling, battery management, etc.).[49] Additionally, there are several sources available that report different values for the considered CAM. In most cases, differences are rather small, but in some cases, significant differences can be identified. These are marked correspondingly for special consideration in future assessments. The higher values are used for the assessment in these cases, and the corresponding sources are marked with a +. More details on the estimation of the reversible capacities and potentials of the anode materials are provided in the Supporting Information.

Because of the lower reversible capacity of sodium and HC compared to lithium and graphite, the reversible specific (also called practical or experimental) energy of SIBs is lower than that of LIBs. Highest values are obtained with metallic anodes, which could be realized in all-solid-state batteries. However, the potential and reversible capacity of the anodes (unlike the cathodes) heavily depends on other parameters such as the electrolyte (affecting initial columbic efficiency ICE, SEI formation),[120] the current rate,[121] element doping,[121] and the presodiating procedure.[122] For reducing uncertainties due to variation of anode properties, the anode is disregarded for the following screening, providing CAM-specific results that are not necessarily valid for an entire battery cell. However, the effect of different anodes is evaluated in the sensitivity analysis.

3.3. Calculation of Impacts

3.3.1. Raw Material Criticality

The development of new technologies is often related to the demand for new raw materials and corresponding concerns regarding their availability and supply security. More than 80% of the raw materials needed for the EUs industry and economy are based on imports, of which several are considered as critical raw materials.[39] There is no common standard for raw material criticality assessment but rather several methods and indicators to analyze raw material criticality with varying spatial and technological and socio-economic scopes.[39,123,124] Based on a review and analysis of existing indicators for assessing raw material criticality, the SR for Europe (SR^{EU})[39] is selected, fitting best to the scope of the present screening approach (a comparison of the different alternative indicators is provided in the Supporting Information). The SR^{EU} considers several factors characterizing the risk of a disruption in the supply of a specific material, including supply country mixes, import reliance, supplier countries' governance performance, trade restrictions and agreements, availability and criticality of substitutes, and end-of-life recycling input rate. Being raw material criticality not only associated with SR, but also with absolute availability of materials, we further estimate static reserves for all relevant raw materials as basis for a sensitivity analysis based on current reserves and mining activities from 2019 to 2021 using reports from the United States Geological Survey (USGS).[125,126] Details about the approach and underlying data are provided in the Supporting Information.

The indicators for the single materials on an element level, calculated static ranges, and qualitative resource availability are provided in **Table 3**.

It is worth mentioning that there is a certain difference among the reviewed indicators when comparing the SR scores obtained for the relevant elements (SR USA/Nassar et al.,[127] USGS review/Hayes et al.,[128] and EU Supply[39]). Also, the static ranges do not necessarily reflect the SR, which is explainable by the fact that the first is based on the bottleneck of supply (either extraction or processing), whilst the latter just considers production capacities and available reserves neglecting any other factor. Additionally, the three main countries for mining or processing level are provided in the right column of Table 3.[129] Note that color indications are different for SR^{EU}, as there is a sharp threshold (value one) beyond which raw materials are defined as critical.

3.3.2. Cathode Active Material (CAM) Cost

Typically, raw materials account for up to 80% of the CAM cost.[130] Thus, a major challenge is to gather representative

Table 2. Result for specific energies for different cathode and anode types.

	Theoretic capacity [mAh g^{-1}]	Reversible capacity [mAh g^{-1}]	Aver. Potential [V]	Reversible specific energy [Wh kg^{-1}] (own calculations)			Ref.	Divergence of literature values for reversible capacity
				With-out anode	Li/Na anode	Graphite/HC anode		
Lithium cathode materials								
$LiCoO_2$	274	150	3.9	585	563	402	[50,51]	None
$LiNi_{0.8}Co_{0.15}Al_{0.05}O_2$ (NCA)	279	188	3.7	696	663	445	[51,52]	None
$LiNi_{0.5}Mn_{0.5}O_2$	280	150	3.9	585	563	402	[53,54]	None
$LiNi_{0.33}Mn_{0.33}Co_{0.33}O_2$ (NMC111)	278	150	3.7	592	568	399	[55,56]	None
$LiNi_{0.6}Mn_{0.2}Co_{0.2}O_2$ (NMC622)	276	170	3.7	629	602	416	[55,57]	None
$LiMn_2O_4$ (LMO)	148	115	4.1	472	458	349	[58,59]	None
$LiNi_{0.5}Mn_{1.5}O_4$ (LNMO)	147	126–137	4.7	644	622	458	[60,61]	Small
$LiFePO_4$ (LFP)	170	165	3.45	569	546	379	[62,63]	None
Sodium cathode materials								
Layered oxide materials								
P2-$Na_{0.67}CoO_2$	168	115–123	3.0	369	334	251	[64,65]+	Small
a-$NaMnO_2$	244	185	2.75	509	439	302	+[66,67]	None
ß-$NaMnO_2$	244	190	2.75	523	449	307	[67,68]+	None
$Na_{0.44}MnO_2$	122	80–120	2.8	336	305	229	[69,70]+	Significant
P2-$Na_{0.67}MnO_2$	175	175	2.8	490	426	297	[71]	
P2-$Na_{0.67}Mn_{0.72}Mg_{0.28}O_2$	191	165–220	2.6	572	481	317	+[72,73]	Significant
P2-$Na_{0.67}Mn_{0.95}Mg_{0.05}O_2$	177	175	2.6	455	396	274	[71]	
P2-$Na_{0.67}Mn_{0.5}Fe_{0.5}O_2$	174	190–195	2.75	523	449	307	[74,75]+	Small
O3-$NaMn_{0.5}Fe_{0.5}O_2$	243	110	2.75	303	276	210	[74]	
P2-$Na_{0.67}Ni_{0.33}Mn_{0.67}O_2$	173	161	3.7	596	523	379	[76,77]	None
P2-$Na_{0.8}Li_{0.12}Ni_{0.22}Mn_{0.66}O_2$	214	118–122	3.4	415	376	285	[78,79]+	Small
P2-$Na_{0.83}Li_{0.07}Ni_{0.31}Mn_{0.62}O_2$	214	140	3.5	490	437	324	[78]	
P2-$Na_{0.83}Li_{0.25}Mn_{0.75}O_2$	237	155–185	2.7	500	431	296	+[80,81]	Significant
O3-$NaFe_{0.5}Co_{0.5}O_2$	238	125–160	3.14	502	442	317	+[82,83]	Significant
O3-$NaNi_{0.33}Co_{0.33}Fe_{0.33}O_2$	238	165	2.95	487	426	303	[84]	
O3-$NaNi_{0.5}Mn_{0.5}O_2$	240	125–130	2.9	377	339	252	[85,86]+	Small
$Na_{0.9}[Mn_{0.4}Fe_{0.5}Ti_{0.1}]O_2$	244	110	2.8	308	281	215	[87,88]	None
$NaMn_{0.33}Fe_{0.33}Ni_{0.33}O_2$	240	100–175	2.75	481	418	292	[89,90]+	Significant
$Na_{0.6}Fe_{0.11}Mn_{0.66}Ni_{0.22}O_2$	159	120	2.7	324	294	220	[91]	
$NaMn_{0.3}Fe_{0.4}Ni_{0.3}O_2$	241	130	3.0	390	351	261	[92]	
P2-$Na_{0.6}Fe_{0.2}Mn_{0.65}Ni_{0.15}O_2$	158	200	3.1	620	529	361	[93]	
$Na_{0.6}Ni_{0.22}Al_{0.11}Mn_{0.66}O_2$	164	225	3.0	675	566	375	[94]	
Polyanionic materials								
$Na_3V_2(PO_4)_3$	118	100–112	3.4	381	347	268	[95,96]+	Small
$Na_4MnV(PO_4)_3$	111	110	3.46	380[a)]	347	269	[97]	
$Na_3MnTi(PO_4)_3$*)	117	114	3.60	410[a)]	374	288	[98]	
$Na_3MnTi(PO_4)_3$**)	176	172	2.94	506[b)]	441	310	Own data[98]	
$Na_3MnZr(PO_4)_3$	107	110	3.66	402[b)]	368	285	[99]	
$NaFePO_4$	154	152	2.7	410	363	260	[100]	
$Na_{1.7}O_2Fe_3(PO_4)_3$	87	140	2.9	406	362	265	[89,101]	None
$Na_4Fe_3(PO_4)P_2O_7$**)	152	105–108	3.2	406	362	244	+[102,103]	Small

Table 2. Continued.

	Theoretic capacity [mAh g^{-1}]	Reversible capacity [mAh g^{-1}]	Aver. Potential [V]	Reversible specific energy [Wh kg^{-1}] (own calculations)			Ref.	Divergence of literature values for reversible capacity
				With-out anode	Li/Na anode	Graphite/HC anode		
Na_2MnPO_4F *)	249	120–178	3.66	651	565	400	+[104,105]	Significant
$NaV(PO_4)F$	143	82–98	3.7	303	283	230	[106,107]+	Small
$Na_{1.5}VPO_{4.8}F_{0.7}$	130	134	3.8	509	457	343	[108]	
$Na_2Fe(PO_4)F$	124	110–120	3.0	360	326	246	[109,110]+	Small
$Na_3MnPO_4CO_3$*)	192	125–130	3.7	490	437	324	[111,112]+	Small
$Na_2MnFe(CN)_6$*)	171	103–140	3.5	490	437	324	+[113,114]	Significant
$Na_{0.61}Fe[Fe(CN)_6]_{0.94}$[1)]	61	170	2.9	493	430	303	[115]	
$Na_{0.81}Fe[Fe(CN)_6]_{0.79}$[1)]	90	149	3.0	447	396	287	[34]	
Na_2FeSiO_4*)	276	175–181	4.0	724	627	444	+[88,116]	Small
Na_2MnSiO_4*)	278	210	3.0	630	534	359	[117]	
$Na_2Fe_2(SO_4)_3$*)	120	102–110	3.8	418	382	297	[118,119]+	Small

[a)]Specific energy is directly from the Literature and the average potential is calculated; [b)]Specific energy is calculated from the integration of the potential-capacity; *2Na exchange; **3Na exchange; [1)]Prussian Blue Analogues

values for the CAM precursor materials as the prices of raw materials are subject to high fluctuations. For this purpose, data obtained from several sources have been combined, considering stock exchange markets and commodity summary reports.[131–133]

All prices have been converted to EUR for the last 11 years (2012–2022)[134] and adjusted to the industrial producer's prices index (IIPP for EU 27).[135] In some cases, only prices for certain precursors are available, for example, lithium carbonate, sodium carbonate (soda ash), and vanadium pentoxide, which have then been converted into the specific precursor price via stoichiometric calculations (See Supporting Information).

Apart from raw material costs, CAM costs entail also process-related costs. The baseline cost of CAM production is used from

Table 3. Overview of different criticality indicators applied to the considered Elements and their specific special focus, where red indicates a high, yellow a moderate, and green a low "criticality". Corresponding minimum and maximum values are provided at the very bottom of the table.

Element	EU Supply Risk (SR^{EU})	Nassar et al. Supply Risk	Hayes et al. – USGS Review	Static range [y]	Three main suppliers (int. Country codes) by global share	Level
Scope	Europe	US	Global	Global	Global	
Al	**0.6**	0.6	33	153	CN 55%, RU 5.7%, IND 4,6%	Processing
Co	**2.5**	0.6	73	49	CD 72.4%, AU 3.7%, RU 3.5%	Mining
F	**1.2**	0.3	57	44	CN 52,7%, MX 29.5%, VN 3.6%	Mining
Fe	**0.5**	0.1	25	64	AU 36.8%, BR 19.3%, CN 13.8%	Mining
Li	**1.6**	0.35	40	240	AU 60.9%, CL 19%, CN 7.5%	Mining
Mg	**3.9**	0.4	75	954	CN 90.9%, USA 3.2%, IL 2.2%	Processing
Mn	**0.9**	0.35	40	68	ZA 28%, AU 16.9%, GA 13.6%	Mining
Na	**0**	0	0	1000	N/A	N/A
Ni	**0.5**	0.4	19	38	CN 31.3%, ID 13.2%, JP 8.5%	Processing
P	**1.1**	0.25	40	282	CN 41.1%, MA 15.6%, USA 10.3%	Processing
S	**0.3**	0	0	1000	N/A	N/A
Si	**1.2**	0	20	1000	CN 61.9%, USA 14.8%, BR 6.5%	Processing
Ti	**1.3**	0.4	25	50	ZA 14.8%, MZ 12.8%, AU 11.6%	Mining
V	**1.7**	0.45	67	271	CN 58.7%, RU 18.8%, ZA 16.4%	Mining
Zr	**0.8**	0.2	57	45	AU 32.3%, ZA 29.5%, USA 8.0%	Mining
Min	0	0	0	12		
Max	7	1	100	1000		
Threshold	1	N/A	N/A	N/A		

literature and usually includes the synthesis process cost or CAM preparation cost (CAMPC). Here a distinction in terms of cost can be made between layered oxides and polyanionic materials. Additionally, this price depends on the size of the production plant due to scale factors. In the case of SIBs, large-scale production is not yet established, and production costs can be expected to decrease in the future with larger-scale production.[136] However, CAM preparation for SIB can be assumed to be very similar to those of LIB, with similar synthesis processes for both layered oxides and polyanionic cathode types.[43] Here the values for CAM preparation from literature[44,136] are used and adopted based on the specific nickel content of LIB and SIB as nickel-rich materials need more complex process steps due to complex surface chemistry[137] (see Supporting Information). Surprisingly, little data is available on the CAMPC of polyanionic CAM. Only Wentke et al.[130] provide a value of 10.2 € kg^{-1} CAM, which is used for the calculation for SIB cathode CAMPC. The cost is comparable to that reported in Peters et al.,[43] where a value of 9.15 € kg^{-1} is used (for co-precipitated metal oxides)

Processing costs for established CAM technologies will probably not decrease further over time, meaning that changes in CAM costs are mainly based on changes in raw material pricing and economies of scale but not due to further learning curve effects.[130,138] Here the main scope is on low TRL technology with no industrial line manufacturing, but the effect of assuming large-scale production (35 GWh production line) is evaluated in the sensitivity analysis.[130] The high fluctuations of raw material costs add significant uncertainty to the CAM cost assessments. To consider these, a Monte-Carlo simulation is used for determining median values and 5%–95% confidence intervals for all raw material process, thus better capturing the associated uncertainties. This is combined with a simple geometric Brownian motion model (GBM) for also considering potential future price developments and the additional uncertainty. Details about the approach are provided in the Supporting Information.

The precursor material costs used for the estimation of CAM costs are presented in **Table 4**. Here only some years of corresponding commodity prices are depicted, the full-time series is provided in the Supporting Information.

3.3.3. Environmental Impacts

Being the CAM and the associated upstream processes (mining, beneficiation, etc.) among the main contributors to the environmental impacts of LIB and SIB,[4,14] a screening of potential impacts in the early design stage can help to support the design of more environmentally friendly batteries. For this purpose, an LCA approach is taken, estimating the potential environmental impacts of the considered material precursors including all upstream processes and the impacts of material synthesis. For the latter, only energy demand (heat and electricity) are taken into account, disregarding infrastructure and possible auxiliary inputs, being no information available on specific requirements of each of the considered CAM, and the impact of auxiliary input for CAM synthesis is typically negligible.[14,45] For layered oxide CAM, electricity and heat demand (process heat from natural gas) are assumed to be 6.87 kWh and 39.6 MJ per kg of CAM produced, respectively, and for polyanionic CAM, these are 6.87 kWh and 15.6 MJ.[4,142] CAM synthesis is assumed to take place in Europe, relying on the corresponding average electricity mix. The screening is based on the ecoinvent database version 3.8, with the impacts for the market mix of each material precursor calculated using the Environmental Footprint (EF) 3.0. impact assessment methodology as recommended

Table 4. Raw material prices with normalized values and used prices for CAM evaluation.

Commodity	Year	Market price [€ t^{-1}]					EUR [kg]			Market price
		2012	2017	2021	2022*	Precursor (converted)	Min	Median	Max	Source
Aluminum	Al	1611	1752	2096	2542	Aluminum Sulfate	1.4	1.6	2.1	[132,133,139,140]
Graphite	C	963	756	972	N/A	Graphite	0.6	0.8	1.1	[132,133,139]
Cobalt	Co	24 281	43 089	48 878	73 729	Cobalt Sulfate	21.2	27.0	49.6	[132,133]
Fluorspar	F	N/A	236	338	N/A	Fluorspar	0.4	0.6	0.7	[140]
Iron Ore (62%)	Fe	102	64	137	130	Iron sulfate	0.2	0.4	0.6	[140]
Lithium carbonate	Li	3360	8101	14 941	59 322	Lithium carbonate	14.8	35.3	315.8	[131–133]
Magnesium	Mg	1925	1954	3415	N/A	Magnesium Sulfate	1.7	1.9	3.4	[132,133,141]
Manganese	Mn	N/A	1595	3329	N/A	Manganese Sulfate	1.4	1.7	3.3	[133,140]
Sodium carbonate	Na	156	146	288	N/A	Sodium carbonate	0.2	0.4	0.6	[131,132]
Nickel	Ni	13 969	9262	15 648	27 119	Nickel Sulfate	8.5	12.4	16.5	[132,133,139,140]
Phosphate	P	147	80	104	N/A	Phosphate	0.2	0.3	0.5	[132,133,140]
Sulfur	S	99	125	200	N/A	Sulfur	0.0	0.1	0.3	[132]
Ferrosilicon (75%)	Si	2157	2128	3031	N/A	Ferrosilicon (75%)	2.1	2.8	4.0	[133,140]
Titandioxide	Ti	2890	2584	2771	N/A	Titandioxide	2.8	4.1	4.8	[132,133]
Vanadium Pentoxide	V	20 380	27 972	29 042	15 254	Vanadium Pentoxide	16.4	19.8	69.3	[132,133,140]
Zirkon	Zr	2110	917	1215	N/A	Zirkon	0.9	1.2	2.7	[132,133]

Table 5. GHG emissions associated with precursor material production and CAM synthesis.

CAM Precursor materials	CF [$kgCO_2eq\ kg^{-1}$]	CAM synthesis process	CF [$kgCO_2eq\ kg^{-1}$]
Vanadium pentoxide	30.22	Layered oxide CAM	4.77
Lithium carbonate	7.78	Polyanionic CAM	3.52
Cobalt sulfate	24.81		
Nicken sulfate	7.77		
Magnesium sulfate	1.05		
Iron sulfate	0.16		
Manganese sulfate	0.82		
Sodium sulfate	0.69		
Titanium dioxide	4.9		
Aluminum sulfate	0.59		
Phosphate	1.5084		
Sulfur	0.13		
Fluorspar	0.17		
Zircon	0.61		
Ferrosilicon	8.47		
Graphite	1.68		

by the EC.[143] In order to limit complexity, only the CF is considered as an impact category, being greenhouse gas (GHG) emissions and resource depletion the impact categories with the highest relevance for LIB,[144] and being resource aspects already considered in the criticality screening. **Table 5** provides the GHG emissions obtained by this for the considered CAM precursors and the CAM synthesis process. More detail about other environmental impacts can be found in the Supporting Information.

4. Results

4.1. CAM Criticality

The results for all considered CAM using the SR^{EU} indicator are provided in **Figure 3**. Due to the high dependency of the results on the specific indicator and its spatial scope, results are contrasted to those for other indicators with a different spatial scope in the Supporting Information and the sensitivity analysis. Only the results without anode are considered, the ones for HC, graphite, and metal anodes are analyzed in the sensitivity analysis. The red line represents the benchmark for NMC, and the dashed red line for LFP. Independent of the specific cell chemistry (SIB or LIB), the main drivers for criticality are i) the CAM energy density, ii) the share of critical elements within the CAM (Table 4) and iii) the origin of the raw materials. Polyanionic LIB and SIB CAM perform well in relation to oxide materials. In more detail, LFP for LIBs (also considered as reference), but also Prussian blue analogs and silicon-containing options for SIB show a good performance and could outperform the LIB references. The recycled input ratio (EOL-RIR) values, displayed in the Supporting Information, provide an idea of the recyclability and thus potential circularity of the CAM. Here it is worth mentioning, that low recyclability values are obtained for most well-performing CAM due to the low (economic) recycling incentives for abundant and low-cost materials (unattractive business cases for recycling).

The left graph of Figure 3 indicates the absolute risk score for each element, whilst the right graph depicts the relative contribution of each element to the total score. Here, sodium does not contribute to the criticality as it is considered to be available nearly unlimitedly.[39,126,129] Lithium in contrast, with reserves and production capacities concentrated in South America and Australia, shows a relevant contribution to the total CAM criticality.[145,146] In addition, lithium is currently not yet recycled in significant shares, though this may change in the future.[45,146] Cobalt and vanadium have the highest contribution to the total criticality score due to the strong concentration of mining and refining capacities in DR Congo and China (cobalt) and China (vanadium).[125,126,129] Regarding recycling, current recovery rates for cobalt in Europe are around 22% (on average),[39] but are expected to increase to up to 95% in the future,[147] while recovery rates of vanadium in Europe hardly exceed 2% nowadays.[39] Nickel, relevant for most layered oxide CAM has a low SR value (0.5) but high economic value, mined in different regions such as Indonesia (36%) and the Philippines (13%),[126] whilst processing is dominated by China (31%).[129] Recycling rates are around 17%[39] but are also expected to reach 95% in the future.[147] Similarly, Manganese, relevant for the magnitude of the considered layered oxides but also polyanionic SIB CAM, is not considered to have a high SR but high economic importance, being supplied by south Africa, Gabun, and Australia.[129,148] However, manganese-based CAM tends to have lower energy densities, which can lead to a high score due to increased total material demand. Manganese recycling rates are relatively low (8%)[148] and it is mainly recovered with iron from steel slag.[126] Phosphorous has a similar impact on CAM criticality (with 3.5 for SR),[39] with main mining capacities in China (39%–41% excluding small mines),[126,129] and major reserves

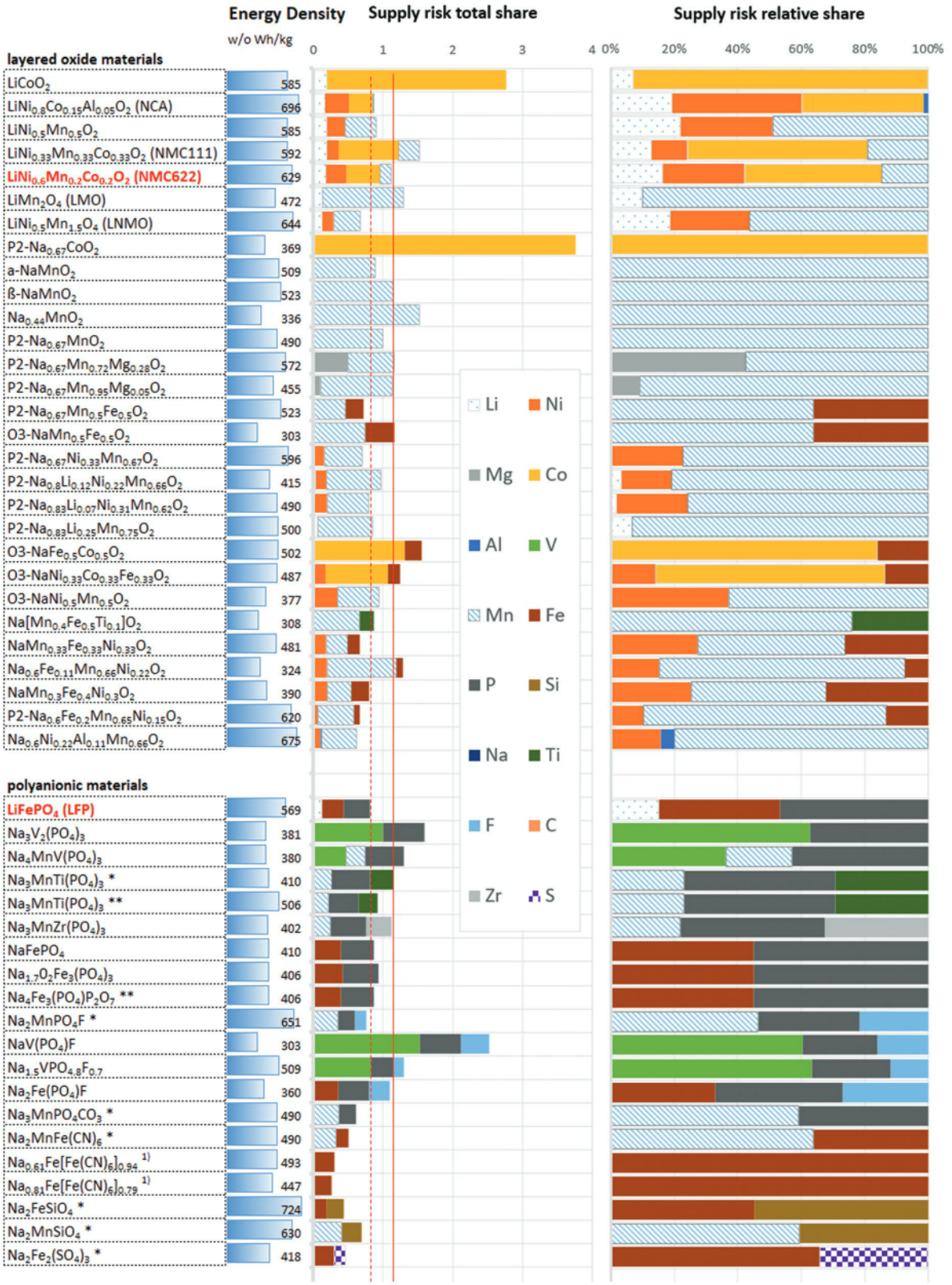

Figure 3. Detailed analysis of the criticality of CAM based on the SR^{EU} indicator (left side) and the relative shares for each cathode type (right side), energy density is provided in form of the blue bars. Indications: a) specific energy is directly from the Literature and the average potential is calculated b) specific energy is calculated from the integration of the potential-capacity, *2Na exchange, **3Na exchange, 1) Prussian Blue Analogues Detailed analysis of criticality of CAM based on the SR^{EU} indicator (left side) and the relative shares for each cathode type (right side).

(75%) in Morocco.[149] Currently, there is no relevant recovery of phosphorus in the EU. Iron plays an important role for SIB, in particular Prussian blue analogs, but also LFP-LIB. Being an abundant element with widely distributed production capacities[126] it has a low SR (0.5), but high economic importance (6.2). Recovery rates for iron are about 31%.[39]

4.2. CAM Cost

The estimated CAM costs (as for CAM criticality for the case w/o anode) are depicted in **Figure 4**. Error bars for CAM cost show the 5%–95% percentile confidence interval, wherein median values are used as a base for comparison. As for criticality, the red line represents the benchmark for NMC, and the dashed red line for LFP. It can clearly be seen that in all cases the raw material cost is significantly lower in relation to the LIB reference (NMC622) under the given assumptions (left graph). The corresponding share of CAM cost of every material for each cathode type is provided in the right graph of Figure 4. While lithium contributes a relevant share to the total CAM costs for LIB, the contribution of sodium to the cost of SIB CAM is almost negligible. Cobalt, nickel, and vanadium can clearly be identified as principal cost drivers for CAM, being these are also the raw materials with the highest price fluctuations.

Vanadium sourced as a byproduct of vanadiferous iron is highly dependent on steel production rates (dominated by China) with corresponding fluctuations, for example, 15–69 USD kg^{-1} over the last 4 years (see Supporting Information). Cobalt prices have been increasing in particular in the last three years with prices of 60–86 USD kg^{-1} due to increasing demand from the battery sector. Currently, prices are not expected to fall due to ongoing disturbances of raw material supply and reduced activity of intermediate product smelters in China.[150] However, cobalt prices have the highest impact on both, LIB and SIB. The results for cobalt-containing SIB cathodes are in a similar magnitude to those reported in literature,[46] in particular $NaNi_{1/3}Co_{1/3}Mn_{1/3}O_2$ if reduced energy densities are considered in the case of an entire cell. Nickel prices have been relatively stable 9000–15 500 USD t^{-1} from 2010 to 2021, but peaked significantly due to increased demand as well as the war in Ukraine (over 45 000 USD t^{-1} depending on the trading platform) and are now decreasing again due to lower demand (by now 26 000 USD t^{-1}).[151] Li_2CO_3 prices have increased from 15.000 USD t^{-1} in June 2021 to 68 800 USD t^{-1} in June 2022, with a slightly declining trend since then. A reason for this is that the demand for lithium has increased while the supply channels are not smooth but are expected to stabilize over time on a high level.[152] While iron phosphate cost is relatively low, cross-checking the calculated with current prices provided by Shanghai Metal Market (SMM) shows that prices have been increasing significantly from 2000 USD t^{-1} in June 2021 to 3692 USD t^{-1} in June 2022.[131] However, costs might also be driven by phosphate/phosphorous acid costs (wet or dry routes)[153] and the energy-intensive drying process in the $FePO_4$ production process.[154] The same comes true for Prussian blue additives where $FeSO_4$ can be used as a precursor, which has to be produced over several steps (nucleation, enlargement of formed crystals, aggregation of formed crystals, and, finally, recrystallization, further oxidation, rinsing of impurities and drying).[155] Iron prices have been very stable in the analyzed time frame with a peak in 2021 and are expected to stay stable.

However, it has to be considered that CAM costs do not necessarily reflect cell battery cell costs, with a substantial share of the cell costs being related to investment, auxiliaries, and overhead costs, which also scale with energy density. Therefore, cost estimations including CAMPC are provided for all considered CAM. These results are based on a bottom-up approach using raw material prices for estimating the corresponding precursor cost, an approach considerably simpler than other cost models from example.[130,137,156] Nevertheless, they are considered to be appropriate for an early-stage screening where little information is available on industrial synthesis processes (and corresponding costs). While the results obtained for LIBs here are in the same order of magnitude as those reported in literature for NMC or LFP against graphite,[130,157] they are just a first explorative screening of potential cost for cathode processing. For a more robust decision-making, a more detailed cost analysis needs to be carried out for each specific material and corresponding synthesis routes.

CAMPC differs between the polyanionic and layered oxides, with a value of 10.2 € kg^{-1} assumed for polyanionic CAM (based on data for LFP) and 6–8.5 € kg^{-1} for layered oxides (derived from data for NMC). These can be explained by different electrode coating thicknesses,[130] with more energy required for coating and drying thicker electrodes, leading to increased cost.[158] The cost for layered oxides is mainly driven by the raw materials (and therefore highly dependent on the energy density), while those for polyanionic CAM are driven by the CAMPC.[156] Therefore, despite having polyanionic CAM potentially lower material costs, their higher CAMPC can compensate for their cost advantage on material level, leading to comparable costs when considering production costs.[137] It is important to mention that cost on a cell level can vary significantly and lead to a very different picture.[159]

4.3. CAM Carbon Footprint

As for cost, an overview of the CF for different CAM is provided in **Figure 5**. Remarkably, the overall picture is very similar to that obtained for the CAM costs, indicating that costs could be considered a fair proxy for GHG emissions for the given approach and assessed technology. While energy density is one of the keys for a good environmental performance, also material choices play an important role, with cobalt and vanadium-containing CAM showing disadvantages due to potentially high environmental impacts from material mining and processing. Also, nickel contributes significantly to the total GHG emissions of CAM production, making the vanadium-free polyanionic CAM and the manganese-based (and nickel and cobalt-less) layered oxides promising candidates under environmental aspects.

As for cost, the results do not represent a full and detailed assessment of the CF related to the different cathodes but

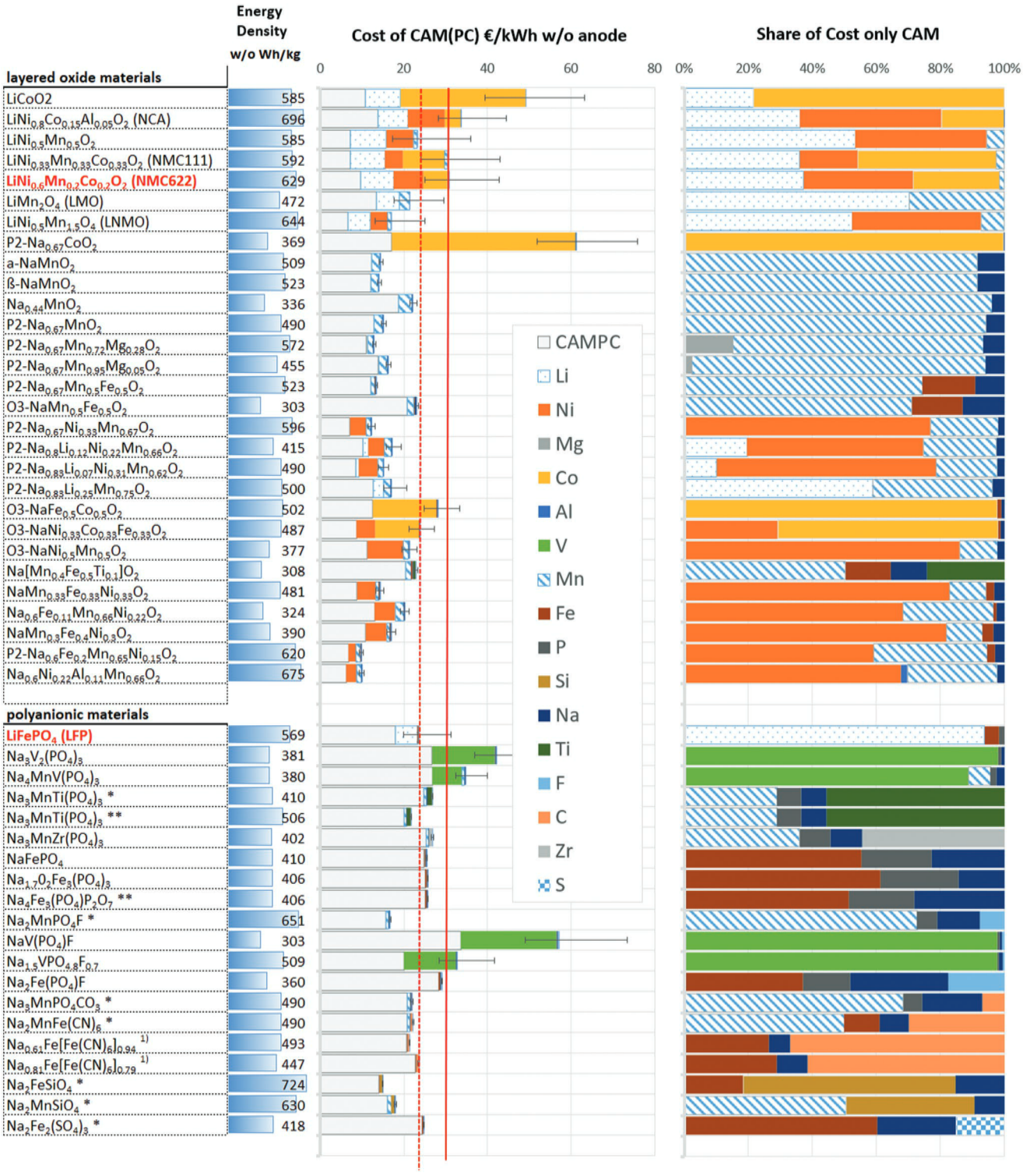

Figure 4. Detailed analysis of CAM Cost in dependence of gravimetric energy density (left side) and the relative shares for each cathode type (right side) CAM and CAM-Preparation Cost for the considered cathode types. Error bars indicate upper and lower boundaries (5 and 95% Percentiles). Indications: a) specific energy is directly from the Literature and the average potential is calculated b) specific energy is calculated from the integration of the potential-capacity, *2Na exchange, **3Na exchange, 1) Prussian Blue Analogues.

constitute a prospective screening of potential impacts. Any impacts associated with other battery cell materials and cell manufacturing are disregarded, though these might differ between cell chemistries. Taking, for example, LFP as an example, shows that these have higher impacts on a full cell level.[4]

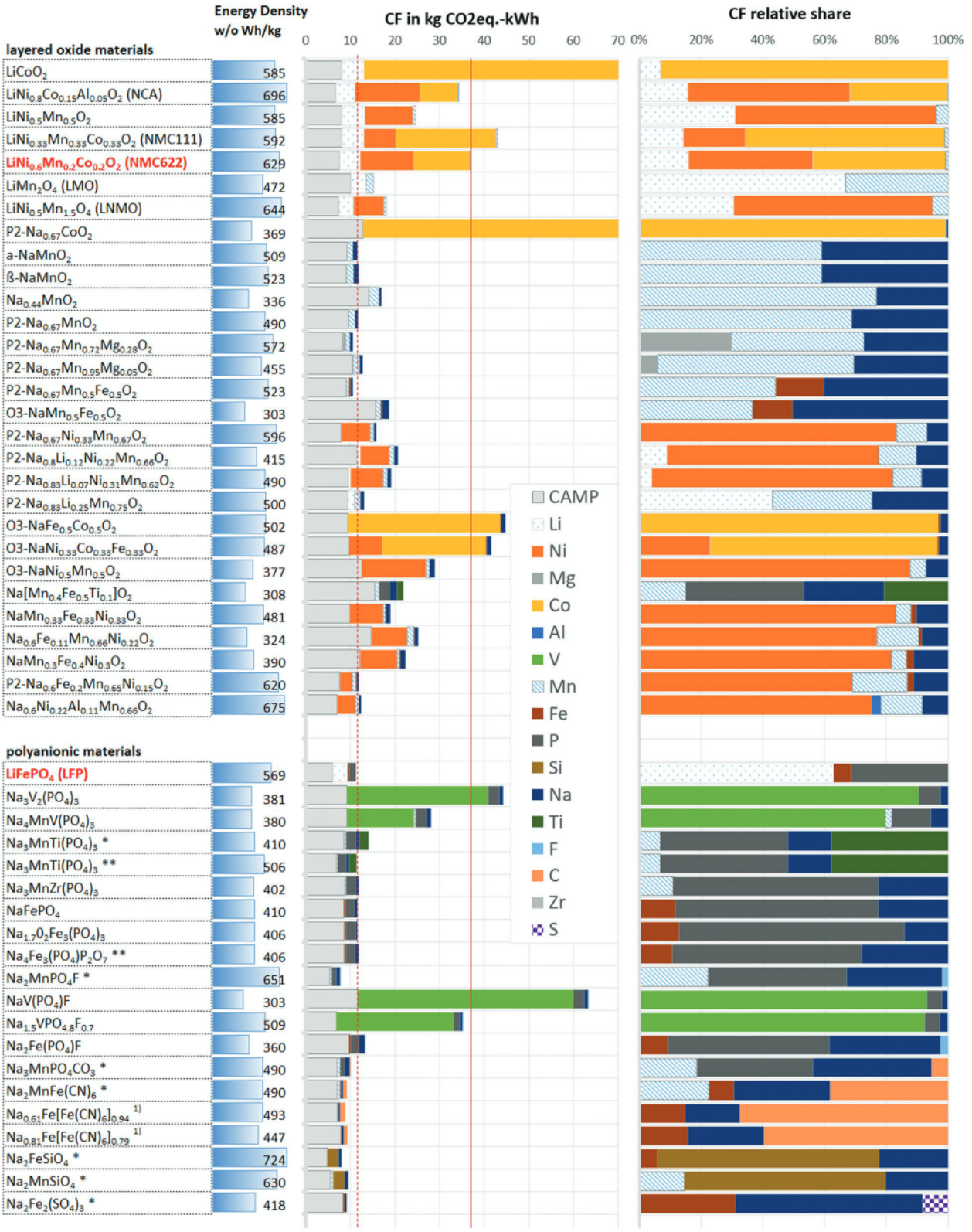

Figure 5. Detailed analysis of CAM Cost in dependence of gravimetric energy density (left side) and the relative shares for each cathode type (right side) CAM and CAM-Preparation Cost for the considered cathode types. Error bars indicate upper and lower boundaries (5 and 95% Percentiles). Indications: a) specific energy is directly from the Literature and the average potential is calculated b) specific energy is calculated from the integration of the potential-capacity, *2Na exchange, **3Na exchange, 1) Prussian Blue Analogues.

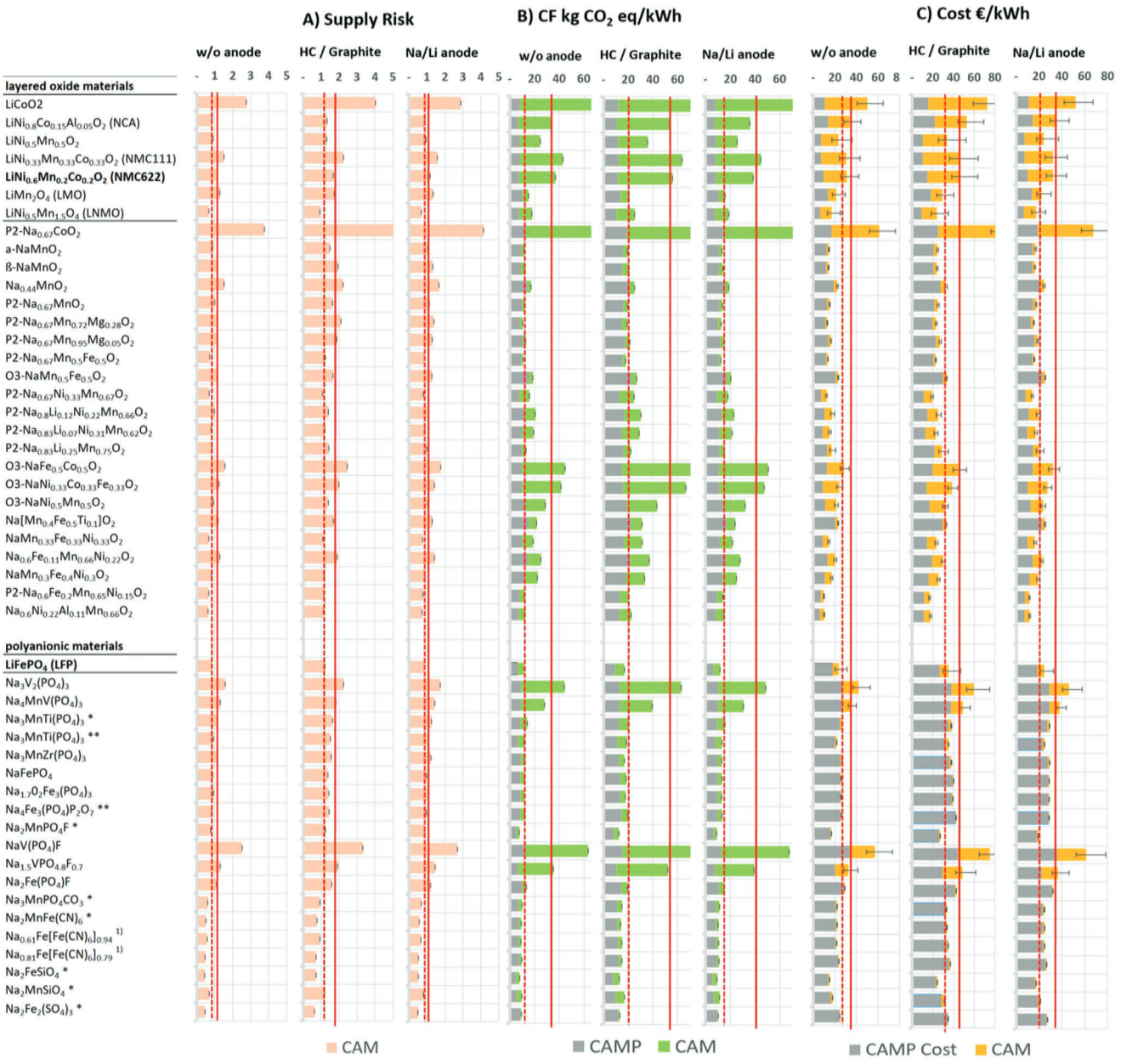

Figure 6. Sensitivity analysis for differing anode materials and changing energy densities for all considered criteria A) SR, B) CF, and C) Cost. Error bars indicate upper and lower boundaries (5 and 95% Percentiles), Indications: a) specific energy is directly from the Literature and the average potential is calculated b) specific energy is calculated from the integration of the potential-capacity, *2Na exchange, **3Na exchange, 1) Prussian Blue Analogues.

5. Sensitivity Analysis

The sensitivity analysis is carried out for i) varying energy densities obtained with different anode types ii) changing prices of the considered raw materials w/o anode using a simple GBM model for material price forecasting for 2031, iii) changing production capacities to analyze potential effects of scale for CAMPC and CAM cost, and iv) contrasting the SR results with those using alternative indicators. The results of the sensitivity analysis are provided in **Figure 6** and **Figure 7**. Again, the red line represents the benchmark of NMC 622 and the dashed one LFP.

The cost and CF estimations include cathode active material preparation efforts (CAMPC) and are provided for all cathode types and three anode options (without anode, metallic, and HC/graphite anode) in Figure 6 A–C. Error bars for cost show the 5%–95% percentile confidence interval for cost in graph C. Again, for cost and CF, the overall picture is very similar with some variation depending on the considered anode type. Higher impacts are obtained for the HC/graphite anodes, while the lowest impacts are obtained without anode, essentially due to the higher specific energy. It has to be mentioned that for some SIB cathodes HC anodes are not applicable. These are all variations where the reversible capacity is higher than the

Figure 7. A) Impact of changing raw material cost for 2032 in comparison to used cost using a simple GBR forecast model (left graph) and B) impact of varying production scales of 1 GWh a^{-1} versus 32 GWh a^{-1} on CAM cost and CAMPC, C) contrasts the SR^{EU} value to other criticality studies for the US, a global scale and static ranges.

theoretical (see Table 2). That means that Na concentration in the host structure is increasing during the first electrochemical cycle. This is possible when more available Na-ions are present in the cell system, for example, due to cycling against sodium metal, presodiating, and sacrificial additives.[160] The values in Figure 6 are therefore underestimated, since all actions to increase the sodium content consume energy, materials, and time which leads to higher costs. However, a common path is not foreseeable, so the values in Figure 6 do not consider these effects. The sensitivity regarding SR (graph A) does not consider CAM production, with the production process assumed to have a negligible impact on total material SR. Also, here, changing specific energies impacts the SR due to increased material demand of lower energy density CAM. However, the overall tendency is the same in all cases, with vanadium-free polyanionic types performing well in relation to layered oxide materials.

The impacts of possible future raw material price developments based on the GBM forecast model for 2031 are shown in Figure 7 A. CAM costs for all cathode materials are predicted to increase for all types in the next 10 years. Depending on the required raw materials, materials CAM price increases of 110%–576% can be expected until 2031. In general, the price volatility of all considered raw materials, in particular, those that are already expensive such as cobalt, nickel, and lithium can be expected to further increase over the course of time.[150,152] This is especially relevant for all LIBs and cobalt-containing SIB, where significant price increments may take place. SIB, despite increasing raw material prices, shows competitive development in relation to LIBs on a CAM cost level. However, here

the CAMP cost has to be considered and have to be analyzed in detail for each chemistry as these can contribute a high share to the total costs, potentially compensating for lower material cost.

As explained before, there are significant economy-of-scale effects for raw material costs. Prices for bulk orders and long-term supply contracts can be up to 30% lower in relation to short-term commodity prices which have been used in the assessment.[130] Also, CAMPC is influenced by the assumed production rates and decreases with a larger scale. Potential impacts on CAM production cost and CAMPC considering 32 GWh/year production plant output (instead of the 1 GWh/year of the baseline) are displayed in Figure 7 B (w/o anode). Larger scale production can lead to CAM cost reductions of up to 50% depending on the analyzed chemistry and materials. Again, the results are only indicative assuming comparable production as well as scale-up effects of SIB in relation to LIB, with other possible factors being disregarded.

Finally, the SR from an EU perspective (SR^{EU}) is contrasted with that of other indicators reviewed (SR USA/Nassar et al.,[127] SR USGS review/Hayes et. al,[128] and static ranges) in Section 3.3.1 (See Figure 7C). All indicators are normalized to a common range (1–100) for better comparability. Most of the used criticality indicators show a similar picture, though the individual criticality values for each CAM vary. Only the static range indicator gives a slightly different picture, with a higher weight / lower availability given to iron, manganese, and fluor, considered rather uncritical by the other indicators (mining vs reserves). This leads to higher impacts for some CAM such as iron cyanide, or iron sulfate-based ones, considered promising by the other indicators. Polyanionic LIB and SIB CAM perform generally well in relation to oxide materials though again, energy density is one of the key factors for a low SR score.

6. Tentative CAM Ranking

A tentative ranking for the screened CAM (w/o anode) allows to determine which materials are the most promising ones under consideration of the three impact categories SR^{EU}, CF, and cost as criteria. There are several multicriteria decision-making methods available that have been used for energy assessment of battery storage technologies.[161] Here, a simple weighted sum method (WSM) is applied to have a transparent calculus, important due to the very high intrinsic uncertainty of the present screening approach on low BTRL. Five different weightings are applied: I) equal weighting (33.3%) for all criteria, ii) focus on environment, with 50% on CF and 25% on SR and Cost (€) each, iii) focus on SR, with 50% on SR, and 25% for CF and cost, iv) focus on cost with 50% on cost and 25% on CF and SR and finally v) equal weights of 25% but with specific energy as fourth, additional criterion. The obtained CAM ranking is provided in **Figure 8**. The WSM scores are very close for some cathode types making it difficult to determine a robust ranking, especially under consideration of the high uncertainties associated with the early-stage screening approach. However, the tentative ranking is provided in grey and gives some orientation to distinguish between the group of promising and not or less promising options in the early development phases.

Most SIB CAM obtain a better score in relation to the NMC 622 reference, with polyanionic materials performing particularly well in relation to current state of art LIB technologies. This comes especially true for Prussian Blue Analogues as well as Si and S containing SIBs. All Cobalt and Vanadium-containing materials are ranked lower, with high associated CF, costs, and SR. Noteworthy is the low variation in the overall ranking when applying different weights to the considered criteria. Adding specific energy as a criterion results in very different rankings. In some cases, as, for example, $Na_2Fe_2(SO_4)_3$ scores are significantly lower. This, however, represents a double accounting of the specific energy which implicitly is already included in the calculus for SR, CF, and Cost. Additional sensitivity analyzes with varying weights including specific energy as a criterion are provided in the Supporting Information.

In any case, the very high uncertainties associated with the present screening approach need to be highlighted again, providing a purely indicative picture to identify the most promising candidates. These candidates require a more detailed assessment on the cell level for decision-making. Considering the entire life cycle, cells can perform very differently regarding their cycle and calendric lifetimes, efficiency degrees, or final energy density, and the selection of a suitable cell is also very dependent on the corresponding application field and not only on the criteria presented here.[4] Within the assessment, two different cost scenarios are considered for 2022 and 2031 to reflect potential changes in raw materials cost (see Supporting Information for details), but are found not to have a significant impact on the results.

7. Discussion

As stated in Section 2, the present screening is based on a SAL 1 with a focus on lab scale cells with a BTRL (between 1–7. This makes it challenging to gather data of comparable quality for all considered CAM. The corresponding simplifications and required assumptions lead to a high degree of uncertainty in the results which has to be considered for interpretation. In this sense, the outcomes of the screening should not be used for decision-making, but rather to pinpoint potential hotspots and support further research into battery eco-design.

One of the major uncertainties that have to be considered is the use of theoretical energy densities, which might not reflect the final value of a cell, even if these were calculated against different anode types for both, SIB and the benchmark technology LIB. Here, in the real world, the active material ratio shows also a big difference between LIBs and SIBs. For example, LIBs are commercially available, and the active material ratio at electrode level is already optimized (e.g., 96 wt.%), while SIBs are at laboratory scale where often only 80 wt.% active material is used.[162] At cell level, the CAM ratio for LIBs is 30.6 to 40.8 wt.% for NCM and LMO, respectively.[163] While even for LIBs the deviation on this level is around 10% and depends on targeted application, for SIBs such values are not available. It should also be highlighted that in SIBs the anode is coated on an aluminum foil instead of copper, allowing potential weight and cost savings on the cell level.[4] Also, no final statement

	Variation of Weights								Variation of Criteria	
	Equal		Environ.		Supply		Cost		+ Spec. En.	
Weights	33% CF, 33% €, 33% SR		50% CF, 25% €, 25% SR		25% CF, 25% €, 50% SR		25% CF, 50% €, 25% SR		25% CF, 25% SE, 25% €, 25% SR	
Year	Score	Rank	Score	Rank	Score	Rank	Score	Rank	Score	Rank
$LiCoO_2$	0.22	48	0.24	48	0.24	48	0.20	48	0.34	47
$LiNi_{0.8}Co_{0.15}Al_{0.05}O_2$ (NCA)	0.70	41	0.71	41	0.75	40	0.67	42	0.77	25
$LiNi_{0.5}Mn_{0.5}O_2$	0.77	39	0.79	39	0.79	38	0.74	39	0.75	28
$LiNi_{0.33}Mn_{0.33}Co_{0.33}O_2$ (NMC111)	0.59	46	0.61	46	0.61	46	0.56	46	0.62	44
$LiNi_{0.6}Mn_{0.2}Co_{0.2}O_2$ (NMC622)	0.66	43	0.68	43	0.70	43	0.63	45	0.70	35
$LiMn_2O_4$ (LMO)	0.83	35	0.86	35	0.81	35	0.83	35	0.73	31
$LiNi_{0.5}Mn_{1.5}O_4$ (LNMO)	0.85	32	0.87	34	0.88	26	0.84	34	0.85	7
P2-$Na_{0.67}CoO_2$	0.00	49	0.00	49	0.00	49	0.00	49	0.04	49
a-$NaMnO_2$	0.92	15	0.94	14	0.91	14	0.94	13	0.82	15
ß-$NaMnO_2$	0.89	23	0.92	23	0.87	27	0.92	21	0.81	18
$Na_{0.44}MnO_2$	0.85	34	0.88	31	0.81	36	0.87	31	0.66	38
P2-$Na_{0.67}MnO_2$	0.91	17	0.93	16	0.90	20	0.93	18	0.80	19
P2-$Na_{0.67}Mn_{0.72}Mg_{0.28}O_2$	0.89	22	0.92	21	0.87	29	0.92	20	0.84	11
P2-$Na_{0.67}Mn_{0.95}Mg_{0.05}O_2$	0.89	24	0.92	22	0.87	28	0.91	22	0.77	24
P2-$Na_{0.67}Mn_{0.5}Fe_{0.5}O_2$	0.94	7	0.96	7	0.94	7	0.96	7	0.85	8
O3-$NaMn_{0.5}Fe_{0.5}O_2$	0.89	26	0.92	24	0.87	30	0.91	23	0.68	36
P2-$Na_{0.67}Ni_{0.33}Mn_{0.67}O_2$	0.90	21	0.91	26	0.91	16	0.90	26	0.85	6
P2-$Na_{0.8}Li_{0.12}Ni_{0.22}Mn_{0.66}O_2$	0.85	33	0.87	33	0.85	33	0.85	33	0.71	34
P2-$Na_{0.83}Li_{0.07}Ni_{0.31}Mn_{0.62}O_2$	0.87	30	0.89	30	0.88	23	0.87	32	0.77	22
P2-$Na_{0.83}Li_{0.25}Mn_{0.75}O_2$	0.90	19	0.92	19	0.90	19	0.91	25	0.80	20
O3-$NaFe_{0.5}Co_{0.5}O_2$	0.64	44	0.65	44	0.65	44	0.65	44	0.61	45
O3-$NaNi_{0.33}Co_{0.33}Fe_{0.33}O_2$	0.69	42	0.69	42	0.71	42	0.68	41	0.63	42
O3-$NaNi_{0.5}Mn_{0.5}O_2$	0.81	37	0.82	37	0.82	34	0.80	37	0.66	40
$Na[Mn_{0.4}Fe_{0.5}Ti_{0.1}]O_2$	0.87	29	0.90	29	0.85	32	0.90	27	0.67	37
$NaMn_{0.33}Fe_{0.33}Ni_{0.33}O_2$	0.89	25	0.90	28	0.91	17	0.89	28	0.78	21
$Na_{0.6}Fe_{0.11}Mn_{0.66}Ni_{0.22}O_2$	0.81	36	0.84	36	0.80	37	0.82	36	0.63	43
$NaMn_{0.3}Fe_{0.4}Ni_{0.3}O_2$	0.87	31	0.88	32	0.88	24	0.87	30	0.71	33
P2-$Na_{0.6}Fe_{0.2}Mn_{0.65}Ni_{0.15}O_2$	0.93	12	0.94	13	0.93	11	0.94	14	0.89	5
$Na_{0.6}Ni_{0.22}Al_{0.11}Mn_{0.66}O_2$	0.92	14	0.94	15	0.93	10	0.93	17	0.92	2
polyanionic materials										
$LiFePO_4$ (LFP)	0.89	27	0.91	25	0.89	21	0.89	29	0.83	13
$Na_3V_2(PO_4)_3$	0.64	45	0.65	45	0.65	45	0.65	43	0.53	46
$Na_4MnV(PO_4)_3$	0.78	38	0.79	38	0.77	39	0.79	38	0.64	41
$Na_3MnTi(PO_4)_3$ *	0.88	28	0.91	27	0.87	31	0.91	24	0.74	30
$Na_3MnTi(PO_4)_3$ **	0.91	16	0.93	17	0.90	18	0.93	15	0.81	16
$Na_3MnZr(PO_4)_3$	0.90	20	0.92	20	0.88	25	0.92	19	0.74	29
$NaFePO_4$	0.93	10	0.95	10	0.92	12	0.95	9	0.77	23
$Na_{1.7}0_2Fe_3(PO_4)_3$	0.92	13	0.94	12	0.91	15	0.95	12	0.76	27
$Na_4Fe_3(PO_4)P_2O_7$ **	0.93	11	0.94	11	0.92	13	0.95	10	0.77	26
Na_2MnPO_4F *	0.94	8	0.96	8	0.94	9	0.96	8	0.92	3
$NaV(PO_4)F$	0.43	47	0.45	47	0.42	47	0.45	47	0.33	48
$Na_{1.5}VPO_{4.8}F_{0.7}$	0.71	40	0.72	40	0.72	41	0.72	40	0.66	39
$Na_2Fe(PO_4)F$	0.90	18	0.93	18	0.88	22	0.93	16	0.72	32
$Na_3MnPO_4CO_3$ *	0.95	6	0.96	6	0.96	6	0.96	6	0.83	12
$Na_2MnFe(CN)_6$ *	0.96	4	0.97	4	0.97	4	0.97	5	0.84	9
$Na_{0.61}Fe[Fe(CN)_6]_{0.94}$ [1)]	0.96	5	0.97	5	0.96	5	0.97	4	0.84	10
$Na_{0.81}Fe[Fe(CN)_6]_{0.79}$ [1)]	0.97	2	0.98	2	0.98	2	0.98	2	0.82	14
Na_2FeSiO_4 *	0.97	3	0.98	3	0.98	3	0.98	3	0.98	1
Na_2MnSiO_4 *	0.94	9	0.95	9	0.94	8	0.95	11	0.90	4
$Na_2Fe_2(SO_4)_3$ *	0.98	1	0.99	1	0.99	1	0.99	1	0.81	17

Figure 8. Explorative score and ranking of cathodes using weighted sum for different scenarios.

can be made about the lifetime of SIB which can lead to very different results depending on the final application and assessment scope. Besides these aspects, there is a fast advancement of CAM synthesis observable, meaning that calculated specific energies can change very fast which has to be considered in future studies.

Second, while the criticality assessment based on SR^{EU} represents the status quo, markets are highly dynamic, especially

for materials experiencing a steep increase in demand due to newly emerging technologies or due to unexpected supply disruptions such as the ones caused by geopolitical developments. SR assessments therefore only provide a snapshot of the current situation and are not necessarily representative for (even near) future situations. Also, the calculation of static ranges is a strong simplification and can change depending on market developments.

Third, also the cost calculus is a simplified approach, assuming the same generic precursors to be used for all CAM production processes. For example, low Ni-containing NMC-type CAMs typically utilize Li_2CO_3, while NMC622 and higher use LiOH[136] which is not considered here. In consequence, cost might be overestimated as they refer to wholesale market prices for high-purity metals. In other cases, this might also lead also to an underestimation of cost if, for example, higher purity materials are required than those typically traded on commodity markets. For CF, similar limitations apply, with only a limited set of precursor materials considered while in reality a more diverse set of precursor materials might be used. Also, the CF of each raw material is estimated as a generic average for the European market, while different manufacturers might source their material from different countries with potentially varying GHG intensity of the materials (due to different production routes, but also different GHG intensity of the national electricity mix). Nevertheless, the price and CF tendency derived for the different cathode types allows for identifying potential hotspots and the need for further refinement of the assessment. Besides the CAM cost, also increasing energy costs might influence CAMPC, due to higher costs for single process steps. Thus, more detailed assessments should be carried out for single chemistries in future studies.

The aspect of recycling can also have a significant impact on the results, in particular favoring LIB chemistries, especially when considering expected progress in hydrometallurgical recycling where the magnitude of materials may be recovered and reused (already with recovery rates over 90%). This is not necessarily a closed loop recycling but may offer significant potential for reducing the impacts of LIBs further. In contrast, the use of abundant materials such as sodium, iron, or silicon may turn out to be a pitfall as they do not provide a sufficient economic incentive to be recycled. Counterintuitively, this might lead to the situation that emerging battery types might not be more sustainable in contrast to the benchmark systems.[4,45]

Most importantly, the results are just valid for the CAM and do not reflect the cost nor the environmental impact of an entire cell which can be very different due to changes in energy densities, and resulting cell performance. The latter plays a highly important role in later applications, for example, determining lifetimes that might influence the environmental performance of SIB.[4] Such assessments require more effort and are limited to lower number of alternatives.

8. Conclusion

The present assessment provides an overview of the potential hotspots of different SIB cathode active materials (CAM) which are currently on a low battery cell readiness level (BTRL). At this stage, most parameters on cell level are unknown, making it difficult to compare them with lithium-ion batteries (LIB) which are considered as a benchmark technology (NMC 622 and LFP). Thus, we propose to couple the assessment to the BTRL and to use methods corresponding which this development level. The suggested screening approach is applicable to early stage development (BTRL 1–4), focusing only on a certain component, here CAM. A set of three indicators covering costs, material criticality, and CF is used to carry out a screening of promising CAM candidates currently being investigated. The approach allows to identify potential material-related hotspots, namely criticality criteria in particular SR, greenhouse gas emissions, and cost and to identify highly and less promising cathode alternatives.

In general, most SIB show a good performance in relation to the LIB (NMC622 and LFP) benchmark regarding cost, CF, and criticality. A major advantage under all three aspects is the use of sodium instead of lithium. However, other materials have a strong impact on the CAM performance regarding the selected indicators. Here a clear disadvantage is identified for cobalt, nickel, magnesium, and vanadium-containing CAM, while SIB relying on Prussian blue and manganese-based CAM turn out to be promising candidates under the present screening. However, not only materials, but the energy density is one of the most important factors determining the overall material demand of SIBs and thus their potential impacts in terms of cost, CF or criticality.

The criticality assessment shows that most of the screened CAM are labeled as critical. This does not represent their abundance in the earth's crust but is related to potential bottlenecks of supply. A good example is magnesium, for which high resources are available, but processing is highly concentrated. Here, a solution can be to diversify supply chains and to re-establish and re-in force, for example, magnesium production in Europe. Additionally, recycling can play a highly important role to minimize import dependencies in line with SIB production in Europe and to maintain critical materials within the cycle (which comes of course also true for LIB as well).

Based on the proposed screening method, an indicative ranking of the considered SIB CAM can be provided in relation to the reference technologies (LFP and NMC). The group of Prussian blue analogs, together with $NaFe_2(SO_4)_3$ appears to be very promising among the SIB alternatives, with low criticality, CF, and costs. This is in line with present research tendencies, that consider these type of cathode types as highly promising.

While the presented screening approach can serve as a blueprint for assessing early-stage battery systems or even other technologies with low technological maturity, also its limitations need to be taken into account. It is essentially a screening approach and therefore does not allow to derive any precise conclusion on final battery cell performance regarding the considered impact categories. All results need to be considered highly explorative as they inhibit a high degree of uncertainty. Still, it allows to obtain a first and rapid picture of potential hotspots and potentials that need to be considered as a starting point for more detailed follow-up analyzes.

Supporting Information

Supporting Information is available from the Wiley Online Library or from the author.

Acknowledgements

This work contributes to the research performed at CELEST (Center for Electrochemical Energy Storage Ulm-Karlsruhe) and was funded by the German Research Foundation (DFG) under Project ID 390874152 (POLiS Cluster of Excellence, EXC 2154). M.B. and M.W. acknowledge the funding by the European Union's Horizon 2020 Research and Innovation Program under Grant Agreement No. 875126 (StoRIES).

Open access funding enabled and organized by Projekt DEAL.

Conflict of Interest

The authors declare no conflict of interest.

Data Availability Statement

The data that support the findings of this study are available from the corresponding author upon reasonable request.

Keywords

carbon footprint, cost, criticality, lithium ions, sodium ions

Received: August 2, 2022
Revised: September 7, 2022
Published online: October 10, 2022

[1] M. Sawicki, L. L. Shaw, *RSC Adv.* **2015**, *5*, 53129.
[2] W. Zhou, M. Zhang, X. Kong, W. Huang, Q. Zhang, *Adv. Sci.* **2021**, *8*, 2004490.
[3] J. F. Peters, M. Baumann, B. Zimmermann, J. Braun, M. Weil, *Renewable Sustainable Energy Rev.* **2017**, *67*, 491.
[4] J. F. Peters, M. Baumann, J. R. Binder, M. Weil, *Sustainable Energy Fuels* **2021**, 6414.
[5] C. Vaalma, D. Buchholz, M. Weil, S. Passerini, *Nat. Rev. Mater.* **2018**, *3*, 18013.
[6] K. Chayambuka, G. Mulder, D. L. Danilov, P. H. L. Notten, *Adv. Energy Mater.* **2020**, *10*, 2001310.
[7] J. Peters, D. Buchholz, S. Passerini, M. Weil, *Energy Environ. Sci.* **2016**, *9*, 1744.
[8] J.-Y. Hwang, S.-T. Myung, Y.-K. Sun, *Chem. Soc. Rev.* **2017**, *46*, 3529.
[9] C. Delmas, *Adv. Energy Mater.* **2018**, *8*, 1703137.
[10] "TIAMAT", http://www.tiamat-energy.com/ (accessed: April 2021).
[11] "Farardion", https://www.faradion.co.uk/technology-benefits/sustainable-technology/ (accessed: April 2021).
[12] P. Schäfer, Springer Professional, https://www.springerprofessional.de/battery/electric-vehicles/catl-introduces-first-generation-sodium-ion-battery/19604728 (accessed: December 2021).
[13] CATL, "CATL Unveils Its Latest Breakthrough Technology by Releasing Its First Generation of Sodium-ion Batteries", https://www.catl.com/en/news/665.html, (accessed: June 2021).
[14] J. F. Peters, M. Weil, *J. Cleaner Prod.* **2018**, *171*, 704.
[15] T. Liu, Y. Zhang, Z. Jiang, X. Zeng, J. Ji, Z. Li, X. Gao, M. Sun, Z. Lin, M. Ling, J. Zheng, C. Liang, *Energy Environ. Sci.* **2019**, *12*, 1512.
[16] A. M. Skundin, T. L. Kulova, A. B. Yaroslavtsev, *Russ. J. Electrochem.* **2018**, *54*, 113.
[17] J. Liu, W. H. Kan, C. D. Ling, *J. Power Sources* **2021**, *481*, 229139.
[18] Q. Liu, Z. Hu, W. Li, C. Zou, H. Jin, S. Wang, S. Chou, S.-X. Dou, *Energy Environ. Sci.* **2021**, *14*, 158.
[19] Q. Liu, Z. Hu, M. Chen, C. Zou, H. Jin, S. Wang, S. Chou, Y. Liu, S. Dou, *Adv. Funct. Mater.* **2020**, *30*, 1909530.
[20] C. Chen, Z. Han, S. Chen, S. Qi, X. Lan, C. Zhang, L. Chen, P. Wang, W. Wei, *ACS Appl. Mater. Interfaces* **2020**, *12*, 7144.
[21] Y. Deng, Z. Wu, R. Liang, Y. Jiang, D. Luo, A. Yu, Z. Chen, *Adv. Funct. Mater.* **2019**, *29*, 1808522.
[22] T. Jin, H. Li, K. Zhu, P.-F. Wang, P. Liu, L. Jiao, *Chem. Soc. Rev.* **2020**, *49*, 2342.
[23] Z. Gong, Y. Yang, *Energy Environ. Sci.* **2011**, *4*, 3223.
[24] A. K. Padhi, V. Manivannan, J. B. Goodenough, *J. Electrochem. Soc.* **1998**, *145*, 1518.
[25] P. Barpanda, L. Lander, S. Nishimura, A. Yamada, *Adv. Energy Mater.* **2018**, *8*, 1703055.
[26] S. T. Senthilkumar, W. Go, J. Han, L. Pham Thi Thuy, K. Kishor, Y. Kim, Y. Kim, *J. Mater. Chem. A* **2019**, *7*, 22803.
[27] S.-Y. Chung, J. T. Bloking, Y.-M. Chiang, *Nat. Mater.* **2002**, *1*, 123.
[28] J. Li, B. Peng, Y. Li, L. Yu, G. Wang, L. Shi, G. Zhang, *Chem. - Eur. J.* **2019**, *25*, 13094.
[29] L. Si, Z. Yuan, L. Hu, Y. Zhu, Y. Qian, *J. Power Sources* **2014**, *272*, 880.
[30] W. Shen, C. Wang, Q. Xu, H. Liu, Y. Wang, *Adv. Energy Mater.* **2015**, *5*, 1400982.
[31] S. Tao, X. Wang, P. Cui, Y. Wang, Y. A. Haleem, S. Wei, W. Huang, L. Song, W. Chu, *RSC Adv.* **2016**, *6*, 43591.
[32] T. Akçay, M. Häringer, K. Pfeifer, J. Anhalt, J. R. Binder, S. Dsoke, D. Kramer, R. Mönig, *ACS Appl. Energy Mater.* **2021**, *4*, 12688.
[33] L. Wang, J. Song, R. Qiao, L. A. Wray, M. A. Hossain, Y.-D. Chuang, W. Yang, Y. Lu, D. Evans, J.-J. Lee, S. Vail, X. Zhao, M. Nishijima, S. Kakimoto, J. B. Goodenough, *J. Am. Chem. Soc.* **2015**, *137*, 2548.
[34] Y. You, X.-L. Wu, Y.-X. Yin, Y.-G. Guo, *Energy Environ. Sci.* **2014**, *7*, 1643.
[35] NASA, Technology Readniess Level, https://www.nasa.gov/directorates/heo/scan/engineering/technology/technology_readiness_level (accessed: July 2022).
[36] M. Greenwood, J. M. Wrogemann, R. Schmuch, H. Jang, M. Winter, J. Leker, *J. Power Sources Adv.* **2022**, *14*, 100089.
[37] IEC, *Dependability management – Part 3-3: Application guide – Life cycle costing* Geneva, Switzerland **2004**.
[38] G. Rodriguez-Garcia, J. Braun, J. Peters, M. Weil, *Mater. Tech.* **2017**, *105*, 517.
[39] European Commission, Study on the EU's list of Critical Raw Materials – Final Report **2020**.
[40] R. Hischier, N. H. Kwon, J. Brog, K. M. Fromm, *ChemSusChem* **2018**, *11*, 2068.
[41] J. F. Peters, M. J. Baumann, B. Zimmermann, J. Braun, M. Weil, *Renewable Sustainable Energy Rev.* **2017**, *67*, 491.
[42] M. J. Baumann, J. F. Peters, M. Weil, A. Grunwald, *Energy Technol.* **2016**, *5*, 1071.
[43] J. F. Peters, A. Peña Cruz, M. Weil, *Batteries* **2019**, *5*, 10.
[44] M. Wentker, M. Greenwood, M. C. Asaba, J. Leker, *J. Energy Storage* **2019**, *26*, 101022.
[45] M. Mohr, J. F. Peters, M. Baumann, M. Weil, *J. Ind. Ecol.* **2020**, *24*, 1310.
[46] S. F. Schneider, C. Bauer, P. Novák, E. J. Berg, *Sustainable Energy Fuels* **2019**, *3*, 3061.
[47] J. F. Peters, M. Abdelbaky, M. Baumann, M. Weil, *Mater. Tech.* **2019**, *107*, 503.
[48] H. S. Hirsh, Y. Li, D. H. S. Tan, M. Zhang, E. Zhao, Y. S. Meng, *Adv. Energy Mater.* **2020**, *10*, 2001274.
[49] M. R. Palacin, *Acc. Mater. Res.* **2021**, *2*, 319.

[50] J. N. Reimers, J. R. Dahn, *J. Electrochem. Soc.* **1992**, *139*, 2091.
[51] Y. Lyu, X. Wu, K. Wang, Z. Feng, T. Cheng, Y. Liu, M. Wang, R. Chen, L. Xu, J. Zhou, Y. Lu, B. Guo, *Adv. Energy Mater.* **2021**, *11*, 2000982.
[52] S.-M. Bak, K.-W. Nam, W. Chang, X. Yu, E. Hu, S. Hwang, E. A. Stach, K.-B. Kim, K. Y. Chung, X.-Q. Yang, *Chem. Mater.* **2013**, *25*, 337.
[53] T. Ohzuku, Y. Makimura, *Chem. Lett.* **2001**, *30*, 744.
[54] X. Liu, D. Zhang, M. Zhang, Y. Yan, Z. Li, P. Wang, R. Murakami, *J. Phys. Chem. Lett.* **2022**, *13*, 6181.
[55] T. Ohzuku, Y. Makimura, *Chem. Lett.* **2001**, *30*, 642.
[56] M. Müller, L. Schneider, N. Bohn, J. R. Binder, W. Bauer, *ACS Appl. Energy Mater.* **2021**, *4*, 1993.
[57] R. Jung, M. Metzger, F. Maglia, C. Stinner, H. A. Gasteiger, *J. Electrochem. Soc.* **2017**, *164*, A1361.
[58] P. Strobel, A. Ibarra Palos, M. Anne, *J. Power Sources* **2001**, *97–98*, 381.
[59] Y. Jiang, L. Chai, D. Zhang, F. Ouyang, X. Zhou, S. I. Alhassan, S. Liu, Y. He, L. Yan, H. Wang, W. Zhang, *Nano-Micro Lett.* **2022**, *14*, 176.
[60] J. Yang, X. Han, X. Zhang, F. Cheng, J. Chen, *Nano Res.* **2013**, *6*, 679.
[61] J. Liu, M. Yuan, Z. Li, S. Xie, T. Wang, J. Yan, J. Peng, *Ceram. Int.* **2022**, S0272884222030188.
[62] A. K. Padhi, K. S. Nanjundaswamy, J. B. Goodenough, *J. Electrochem. Soc.* **1997**, *144*, 1188.
[63] N. Aguiló-Aguayo, D. Hubmann, F. U. Khan, S. Arzbacher, T. Bechtold, *Sci. Rep.* **2020**, *10*, 5565.
[64] X. Wang, M. Tamaru, M. Okubo, A. Yamada, *J. Phys. Chem. C* **2013**, *117*, 15545.
[65] L. Gao, S. Chen, L. Zhang, X. Yang, *ChemElectroChem* **2019**, *6*, 947.
[66] X. Ma, H. Chen, G. Ceder, *J. Electrochem. Soc.* **2011**, *158*, A1307.
[67] J. Manzi, A. Paolone, O. Palumbo, D. Corona, A. Massaro, R. Cavaliere, A. B. Muñoz-García, F. Trequattrini, M. Pavone, S. Brutti, *Energies* **2021**, *14*, 1230.
[68] J. Billaud, R. J. Clément, A. R. Armstrong, J. Canales-Vázquez, P. Rozier, C. P. Grey, P. G. Bruce, *J. Am. Chem. Soc.* **2014**, *136*, 17243.
[69] F. Sauvage, L. Laffont, J.-M. Tarascon, E. Baudrin, *Inorg. Chem.* **2007**, *46*, 3289.
[70] X. Zhou, A. Zhao, Z. Chen, Y. Cao, *Electrochem. Commun.* **2021**, *122*, 106897.
[71] J. Billaud, G. Singh, A. R. Armstrong, E. Gonzalo, V. Roddatis, M. Armand, T. Rojo, P. G. Bruce, *Energy Environ. Sci.* **2014**, *7*, 1387.
[72] N. Yabuuchi, R. Hara, K. Kubota, J. Paulsen, S. Kumakura, S. Komaba, *J. Mater. Chem. A* **2014**, *2*, 16851.
[73] E. Boivin, R. A. House, M. A. Pérez-Osorio, J.-J. Marie, U. Maitra, G. J. Rees, P. G. Bruce, *Joule* **2021**, *5*, 1267.
[74] N. Yabuuchi, M. Kajiyama, J. Iwatate, H. Nishikawa, S. Hitomi, R. Okuyama, R. Usui, Y. Yamada, S. Komaba, *Nat. Mater.* **2012**, *11*, 512.
[75] D. Darbar, N. Muralidharan, R. P. Hermann, J. Nanda, I. Bhattacharya, *Electrochim. Acta* **2021**, *380*, 138156.
[76] L. Zhonghua, J. R. Dahn, *J. Electrochem. Soc.* **2001**, *148*, A1225.
[77] W. Zuo, F. Ren, Q. Li, X. Wu, F. Fang, X. Yu, H. Li, Y. Yang, *Nano Energy* **2020**, *78*, 105285.
[78] J. Xu, D. H. Lee, R. J. Clément, X. Yu, M. Leskes, A. J. Pell, G. Pintacuda, X.-Q. Yang, C. P. Grey, Y. S. Meng, *Chem. Mater.* **2014**, *26*, 1260.
[79] R. J. Clément, J. Xu, D. S. Middlemiss, J. Alvarado, C. Ma, Y. S. Meng, C. P. Grey, *J. Mater. Chem. A* **2017**, *5*, 4129.
[80] N. Yabuuchi, R. Hara, M. Kajiyama, K. Kubota, T. Ishigaki, A. Hoshikawa, S. Komaba, *Adv. Energy Mater.* **2014**, *4*, 1301453.
[81] Y. Huang, Y. Zhu, A. Nie, H. Fu, Z. Hu, X. Sun, S. Haw, J. Chen, T. Chan, S. Yu, G. Sun, G. Jiang, J. Han, W. Luo, Y. Huang, *Adv. Mater.* **2022**, *34*, 2105404.
[82] H. Yoshida, N. Yabuuchi, S. Komaba, *Electrochem. Commun.* **2013**, *34*, 60.
[83] N. V. Hoang, H. L. T. Nguyen, T. V. Man, L. M. L. Phung, N. D. Quan, *Vietnam J. Sci. Technol.* **2019**, *57*, 198.
[84] P. Vassilaras, A. J. Toumar, G. Ceder, *Electrochem. Commun.* **2014**, *38*, 79.
[85] S. Komaba, N. Yabuuchi, T. Nakayama, A. Ogata, T. Ishikawa, I. Nakai, *Inorg. Chem.* **2012**, *51*, 6211.
[86] L. Zheng, L. Li, R. Shunmugasundaram, M. N. Obrovac, *ACS Appl. Mater. Interfaces* **2018**, *10*, 38246.
[87] D. Yang, J. Xu, X.-Z. Liao, H. Wang, Y.-S. He, Z.-F. Ma, *Chem. Commun.* **2015**, *51*, 8181.
[88] X. Jiang, F. Hu, J. Zhang, *RSC Adv.* **2016**, *6*, 103238.
[89] D. Liu, G. T. R. Palmore, *ACS Sustainable Chem. Eng.* **2017**, *5*, 5766.
[90] Y. Yu, W. Kong, Q. Li, D. Ning, G. Schuck, G. Schumacher, C. Su, X. Liu, *ACS Appl. Energy Mater.* **2020**, *3*, 933.
[91] D. Kim, E. Lee, M. Slater, W. Lu, S. Rood, C. S. Johnson, *Electrochem. Commun.* **2012**, *18*, 66.
[92] N. Yabuuchi, M. Yano, H. Yoshida, S. Kuze, S. Komaba, *J. Electrochem. Soc.* **2013**, *160*, A3131.
[93] D. Yuan, X. Hu, J. Qian, F. Pei, F. Wu, R. Mao, X. Ai, H. Yang, Y. Cao, *Electrochim. Acta* **2014**, *116*, 300.
[94] I. Hasa, S. Passerini, J. Hassoun, *RSC Adv.* **2015**, *5*, 48928.
[95] Z. Jian, L. Zhao, H. Pan, Y.-S. Hu, H. Li, W. Chen, L. Chen, *Electrochem. Commun.* **2012**, *14*, 86.
[96] Z. Yang, G. Li, J. Sun, L. Xie, Y. Jiang, Y. Huang, S. Chen, *Energy Storage Mater.* **2020**, *25*, 724.
[97] P. R. Kumar, A. Kheireddine, U. Nisar, R. A. Shakoor, R. Essehli, R. Amin, I. Belharouak, *J. Power Sources* **2019**, *429*, 149.
[98] T. Zhu, P. Hu, C. Cai, Z. Liu, G. Hu, Q. Kuang, L. Mai, L. Zhou, *Nano Energy* **2020**, *70*, 104548.
[99] H. Gao, I. D. Seymour, S. Xin, L. Xue, G. Henkelman, J. B. Goodenough, *J. Am. Chem. Soc.* **2018**, *140*, 18192.
[100] S.-M. Oh, S.-T. Myung, J. Hassoun, B. Scrosati, Y.-K. Sun, *Electrochem. Commun.* **2012**, *22*, 149.
[101] X. Lin, X. Hou, X. Wu, S. Wang, M. Gao, Y. Yang, *RSC Adv.* **2014**, *4*, 40985.
[102] H. Kim, I. Park, D.-H. Seo, S. Lee, S.-W. Kim, W. J. Kwon, Y.-U. Park, C. S. Kim, S. Jeon, K. Kang, *J. Am. Chem. Soc.* **2012**, *134*, 10369.
[103] L. Zhang, X. He, S. Wang, N. Ren, J. Wang, J. Dong, F. Chen, Y. Li, Z. Wen, C. Chen, *ACS Appl. Mater. Interfaces* **2021**, *13*, 25972.
[104] M. Law, V. Ramar, P. Balaya, *J. Power Sources* **2017**, *359*, 277.
[105] Y. Sui, Z. Shi, Y. Hu, X. Zhang, X. Wu, L. Wu, *J. Colloid Interface Sci.* **2021**, *603*, 430.
[106] J. Barker, M. Y. Saidi, J. L. Swoyer, *Electrochem. Solid-State Lett.* **2003**, *6*, A1.
[107] C.-D. Zhao, J.-Z. Guo, Z.-Y. Gu, X.-X. Zhao, W.-H. Li, X. Yang, H.-J. Liang, X.-L. Wu, *J. Mater. Chem. A* **2020**, *8*, 17454.
[108] Y.-U. Park, D.-H. Seo, H.-S. Kwon, B. Kim, J. Kim, H. Kim, I. Kim, H.-I. Yoo, K. Kang, *J. Am. Chem. Soc.* **2013**, *135*, 13870.
[109] Y. Kawabe, N. Yabuuchi, M. Kajiyama, N. Fukuhara, T. Inamasu, R. Okuyama, I. Nakai, S. Komaba, *Electrochem. Commun.* **2011**, *13*, 1225.
[110] H. Hu, Y. Wang, Y. Huang, H. Shu, X. Wang, *J. Cent. South Univ.* **2019**, *26*, 1521.
[111] H. Chen, Q. Hao, O. Zivkovic, G. Hautier, L.-S. Du, Y. Tang, Y.-Y. Hu, X. Ma, C. P. Grey, G. Ceder, *Chem. Mater.* **2013**, *25*, 2777.
[112] B. Xie, R. Sakamoto, A. Kitajou, K. Nakamoto, L. Zhao, S. Okada, W. Kobayashi, M. Okada, T. Takahara, *Energies* **2019**, *12*, 4534.
[113] J. Kim, D.-H. Seo, H. Kim, I. Park, J.-K. Yoo, S.-K. Jung, Y.-U. Park, W. A. Goddard III, K. Kang, *Energy Environ. Sci.* **2015**, *8*, 540.
[114] F. Hu, L. Li, X. Jiang, *Chin. J. Chem.* **2017**, *35*, 415.

[115] J. Song, L. Wang, Y. Lu, J. Liu, B. Guo, P. Xiao, J.-J. Lee, X.-Q. Yang, G. Henkelman, J. B. Goodenough, *J. Am. Chem. Soc.* **2015**, *137*, 2658.
[116] B. Ali, A. ur-Rehman, F. Ghafoor, M. I. Shahzad, S. K. Shah, S. M. Abbas, *J. Power Sources* **2018**, *396*, 467.
[117] W. Guan, B. Pan, P. Zhou, J. Mi, D. Zhang, J. Xu, Y. Jiang, *ACS Appl. Mater. Interfaces* **2017**, *9*, 22369.
[118] P. Barpanda, G. Oyama, S. Nishimura, S.-C. Chung, A. Yamada, *Nat. Commun.* **2014**, *5*, 4358.
[119] M. Chen, D. Cortie, Z. Hu, H. Jin, S. Wang, Q. Gu, W. Hua, E. Wang, W. Lai, L. Chen, S. Chou, X. Wang, S. Dou, *Adv. Energy Mater.* **2018**, *8*, 1800944.
[120] L. Shen, S. Shi, S. Roy, X. Yin, W. Liu, Y. Zhao, *Adv. Funct. Mater.* **2021**, *31*, 2006066.
[121] L. Zhao, Z. Hu, W. Lai, Y. Tao, J. Peng, Z. Miao, Y. Wang, S. Chou, H. Liu, S. Dou, *Adv. Energy Mater.* **2021**, *11*, 2002704.
[122] M. Liu, J. Zhang, S. Guo, B. Wang, Y. Shen, X. Ai, H. Yang, J. Qian, *ACS Appl. Mater. Interfaces* **2020**, *12*, 17620.
[123] D. Schrijvers, A. Hool, G. A. Blengini, W.-Q. Chen, J. Dewulf, R. Eggert, L. van Ellen, R. Gauss, J. Goddin, K. Habib, C. Hagelüken, A. Hirohata, M. Hofmann-Amtenbrink, J. Kosmol, M. L.e Gleuher, M. Grohol, A. Ku, M.-H. Lee, G. Liu, K. Nansai, P. Nuss, D. Peck, A. Reller, G. Sonnemann, L. Tercero, A. Thorenz, P. A. Wäger, *Resour., Conserv. Recycl.* **2020**, *155*, 104617.
[124] Y. Jin, J. Kim, B. Guillaume, *Resour., Conserv. Recycl.* **2016**, *113*, 77.
[125] USGS, Mineral Commodity Summaries 2018, US Geological Survey, Reston, Virginia, USA **2019**.
[126] U.S. Geological Survey, Mineral commodity summaries **2022**, p. 202, https://doi.org/10.3133/mcs2022.
[127] N. T. Nassar, J. Brainard, A. Gulley, R. Manley, G. Matos, G. Lederer, L. R. Bird, D. Pineault, E. Alonso, J. Gambogi, S. M. Fortier, *Sci. Adv.* **2020**, *6*, eaay8647.
[128] S. M. Hayes, E. A. McCullough, *Resour. Policy* **2018**, *59*, 192.
[129] S. Al Barazi, et al., DERA – Deutsche Rohstoffagentur In Der Bundesanstalt Für Geowissenschaften und Rohstofffe, DERA-Rohstoffliste, DERA Rohstoffinformationen, Berlin, **2021**, p. 108.
[130] M. Wentker, M. Greenwood, J. Leker, *Energies* **2019**, *12*, 504.
[131] SMM, "Shanghai Metal Market", https://www.metal.com/Ternary-precursor-material/202111010002?type=3%20Years (accessed: June 2022).
[132] T. Kelly, G. Matos, Buckingham, C. DiFrancesco, K. Porter, *U.S. Geol. Surv.* **2022**, 202.
[133] Preismonitor Rohstoffe 2021, *Bundesanstalt Für Geowissenschaften Und Rohstoffe* (BGR), **2021**.
[134] German Bundesbank, https://www.bundesbank.de/dynamic/action/de/statistiken/zeitreihen-datenbanken/zeitreihen-datenbank/723452/723452?tsId=BBEX3.A.USD.EUR.BB.AC.A04&dateSelect=2021 (accessed: January 2022).
[135] Eurostat, http://appsso.eurostat.ec.europa.eu/nui/show.do?dataset=sts_inppnd_a&lang=en (accessed: January 2022).
[136] M. Greenwood, M. Wentker, J. Leker, *J. Power Sources Adv.* **2021**, *9*, 100055.
[137] E. J. Berg, C. Villevieille, D. Streich, S. Trabesinger, P. Novák, *J. Electrochem. Soc.* **2015**, *162*, A2468.
[138] R. Petri, T. Giebel, B. Zhang, J.-H. Schünemann, C. Herrmann, *Int. J. Precis. Eng. Manuf.-Green Tech.* **2015**, *2*, 263.
[139] World Bank, *World Bank Commodities Price Forecast*, World Bank, Washington, DC **2021**.
[140] BGR – Bundesanstalt für Geowissenschaften und Rohstoffe 2021, Deutschland – Rohstoffsituation 2020, Hannover **2021**.
[141] Trading Economics, "Magnesium", https://tradingeconomics.com/commodity/magnesium (accessed: July 2022).
[142] E. Crenna, M. Gauch, R. Widmer, P. Wäger, R. Hischier, *Resour., Conserv. Recycl.* **2021**, *170*, 105619.
[143] S. Fazio, F. Biganzioli, V. De Laurentiis, L. Zampori, S. Sala, E. Diaconu, *Supporting Information to the Characterisation Factors of Recommended EF Life Cycle Impact Assessment Methods: Version 2, from ILCD to EF 3.0*, European Commission, Ispra **2018**, https://doi.org/10.2760/002447.
[144] Recharge **2020**, PEFCR – Product Environmental Footprint Category Rules for High Specific Energy Rechargeable Batteries for Mobile Applications, **2021**.
[145] U.S. Department of Justice and the Federal Trade Commission, *Horizontal Merger Guidelines*, U.S. Department Of Justice And The Federal Trade Commission, Washington, DC **2010**.
[146] BGR, Lithium – Rohstoffliche Steckbriefe, *Bundesanstalt Für Geowissenschaften Und Rohstoffe*, Hannover **2020**.
[147] V. Halleux, *New EU Regulatory Framework for Batteries Setting Sustainability Requirements*, European Parliament, **2022**.
[148] BGR, Mangan – Rohstoffliche Steckbriefe, Bundesanstalt Für Geowissenschaften Und Rohstoffe, Hannover, **2021**.
[149] BGR, Phosphat – Rohstoffliche Steckbriefe, Bundesanstalt Für Geowissenschaften Und Rohstoffe, Hannover, **2014**.
[150] SMM, *A Detailed Analysis of the Reasons Why Cobalt Salt Prices Stopped Falling*, Shanghai Metal Market, Shanghai **2022**.
[151] SMM, *Nickel Shanghai Metal Market*, SMM, Shanghai **2022**.
[152] SMM, *The Rising Lithium Prices Have Been Away from the Fundamentals, and a Mechanism Ensuring the Stability of Lithium Prices Is Expected to be Establish*, Shanghai Metal Market, Shanghai **2022**.
[153] P. Becker, *Phosphates and Phosphoric Acid: Raw Materials, Technology, and Economics of the Wet Process*, M. Dekker, New York **1983**.
[154] X. Si, M. Li, X. Fu, *J. Wuhan Univ. Technol.-Mat. Sci. Ed.* **2019**, *34*, 1097.
[155] A. V. Vyboishchik, M. Y. Popov, *IOP Conf. Ser.: Mater. Sci. Eng.* **2020**, *962*, 022035.
[156] P. A. Nelson, K. G. Gallagher, I. Bloom, D. W. Dees, *Modeling the Performance and Cost of Lithium-Ion Batteries for Electric-Drive Vehicles /BatPaC Model*, Argonne National Laboratory, Chicago **2011**.
[157] W. Bernhart, *The Lithium-Ion (EV) Battery Market and Supply Chain – Market Drivers and Emerging Supply Chain Risks*, Roland Berger, **2022**.
[158] G. Patry, A. Romagny, S. Martinet, D. Froelich, *Energy Sci. Eng.* **2015**, *3*, 71.
[159] S. Sripad, V. Viswanathan, *J. Electrochem. Soc.* **2017**, *164*, E3635.
[160] H. He, D. Sun, Y. Tang, H. Wang, M. Shao, *Energy Storage Mater.* **2019**, *23*, 233.
[161] M. Baumann, M. Weil, J. F. Peters, N. Chibeles-Martins, A. B. Moniz, *Renewable Sustainable Energy Rev.* **2019**, *107*, 516.
[162] M. Armand, P. Axmann, D. Bresser, M. Copley, K. Edström, C. Ekberg, D. Guyomard, B. Lestriez, P. Novák, M. Petranikova, W. Porcher, S. Trabesinger, M. Wohlfahrt-Mehrens, H. Zhang, *J. Power Sources* **2020**, *479*, 228708.
[163] H. Ali, H. A. Khan, M. G. Pecht, *J. Energy Storage* **2021**, *40*, 102690.